https://doi.org/10.5194/cp-2021-122
Preprint. Discussion started: 17 September 2021

Climate of the Past Discussions

Late Paleocene CO_2 drawdown, climatic cooling, and terrestrial denudation in the southwest Pacific

Christopher J. Hollis[1,2], Sebastian Naeher[1], Christopher D. Clowes[1], Jenny Dahl[1], Xun Li[1], B. David A. Naafs[3], Richard D. Pancost[3], Kyle W.R. Taylor[3], G. Todd Ventura[1,4] and Richard Sykes[1]

[1] GNS Science, Lower Hutt, 5040, New Zealand

[2] Victoria University of Wellington, Wellington, New Zealand

[3] Organic Geochemistry Unit, School of Chemistry, School of Earth Sciences, and Cabot Institute for the Environment, University of Bristol, Bristol, UK

[4] Department of Geology, Saint Mary's University, Halifax, Nova Scotia, Canada

Correspondence to: chris.hollis@vuw.ac.nz; s.naeher@gns.cri.nz

Abstract: Late Paleocene deposition of an organic-rich sedimentary facies on the continental shelf and slope of New Zealand and eastern Australia has been linked to short-lived climatic cooling and terrestrial denudation following sea-level fall. Recent studies have confirmed that the organic matter in this facies, termed *Waipawa organofacies*, is primarily of terrestrial origin, with a minor marine component. It is also unusually enriched in $\delta^{13}C$. In this study we aim to determine the cause or causes of this enrichment. For Waipawa organofacies and its bounding facies in the Taylor White section, Hawkes Bay, paired palynofacies and $\delta^{13}C$ analysis of density fractions indicate that the heaviest $\delta^{13}C$ values are associated with degraded phytoclasts (woody plant matter) and that the ^{13}C enrichment is partly due to lignin degradation. Compound specific $\delta^{13}C$ analyses of samples from the Taylor White and mid-Waipara (Canterbury) sections confirms this relationship but also reveal a residual ^{13}C enrichment of ~2.5‰ in higher plant biomarkers (*n*-alkanes and *n*-alkanoic acids) and 3–4‰ in the subordinate marine component, which we interpret as indicating a significant drawdown of atmospheric CO_2.

Refined age control for Waipawa organofacies indicates that deposition occurred between 59.2 and 58.4 Ma, which coincides with a Paleocene oxygen isotope maximum (POIM) and the onset of the Paleocene carbon isotope maximum (PCIM). This timing suggests that this depositional event was related to global cooling and carbon burial. This relationship is further supported by published TEX_{86}-based sea surface temperatures that indicate a pronounced regional cooling during deposition. We suggest that reduced greenhouse gas emissions from volcanism and accelerated carbon burial related to several tectonic factors and positive feedbacks resulted in short-lived global cooling, growth of ephemeral ice sheets, and a global fall in sea level. Accompanying erosion and carbonate dissolution in deep sea sediment archives may have hidden the evidence of this "hypothermal" event until now.

1 Introduction

The Paleocene Epoch (66–56 Ma) is book-ended by the two most extreme biotic and climatic events of the Cenozoic, the Cretaceous–Paleogene mass extinction and the Paleocene-Eocene thermal maximum (PETM; Zachos et al., 2008; Hollis et al., 2019). The intervening ten million years is an intriguing period of Earth system recovery, followed by a progressive warming trend that culminates in the early Eocene with the warmest temperatures of the Cenozoic (Hollis et al., 2019). Deep-sea climate archives indicate that prior to this warming trend, global temperatures reached a minimum between 60–58 Ma (Westerhold et al., 2011, 2020; Littler et al., 2014; Barnet et al., 2019). The relationship between temperature and atmospheric greenhouse gas levels through the Paleocene is very poorly resolved with wide error ranges for both age control

https://doi.org/10.5194/cp-2021-122
Preprint. Discussion started: 17 September 2021

Climate of the Past Discussions
Open Access
EGU

and CO_2 estimates from available proxies (Barnet et al., 2019; Hollis et al., 2019). Nevertheless, global temperature trends through the Paleocene have been linked to factors affecting CO_2 levels, including CO_2 emissions from volcanism (Westerhold et al., 2011), the exhumation (Beck et al., 1995) and burial (Kurtz et al., 2003) of organic carbon due to tectonic processes, and biological productivity (Corfield and Cartlidge, 1992). The interval of peak carbon burial, as indicated by the most positive benthic foraminiferal $\delta^{13}C$ values of the entire Cenozoic, occurred 59–57 Ma and is referred to as the Paleocene carbon isotope maximum (PCIM). This event may have been driven by North American uplift, which led to large epeiric seas being transformed into extensive carbon-sequestering peat deposits (Kurtz et al., 2003). Other studies suggest that changes in ocean circulation caused an increase in marine productivity and oceanic carbon burial, either as a positive feedback to the long-term cooling trend (Corfield and Cartlidge, 1992; Corfield and Norris, 1996) or due to the opening of pathways for deep-water circulation (Batenburg et al., 2018). Climatic cooling may have also resulted in carbon burial as biogenic methane (hydrates) on continental shelves (Dickens, 2003) or within high-latitude permafrost (DeConto et al., 2012). Despite limited and conflicting data for the Paleocene, CO_2 levels in the later Paleogene approach those that we may expect in coming centuries (Foster et al., 2017). Therefore, the discovery of an episode in which extensive carbon burial likely played a major role in climatic cooling warrants investigation as an example of how a geologically brief process can cool the planet by reducing the flux of CO_2 back into the atmosphere. However, the temperature response to the PCIM is poorly understood and in deep-sea records appears to be offset, with most positive benthic foraminiferal $\delta^{18}O$ values at the onset of the PCIM (~59 Ma) rather than the peak (~58 Ma) (Fig. 1). This offset may be related to pervasive deep-sea carbonate dissolution across this 1 Myr interval (Westerhold et al., 2011; Littler et al., 2014), which may distort the benthic foraminiferal oxygen isotope records.

In contrast to these deep-sea records, studies of continental margin sediments in the southwest Pacific reveal evidence for pronounced cooling during the late Paleocene (Contreras et al., 2014; Hollis et al., 2012, 2014) (Fig. 1), which is linked to a fall in sea level and widespread deposition of organic-rich marine sediments (Schiøler et al., 2010). Recent integrated palynofacies and geochemical studies of the distinctive organic matter assemblage in these sediments, named "Waipawa organofacies" by Hollis et al. (2014), revealed it to be primarily of terrestrial origin, comprising mainly degraded wood fragments or phytoclasts (Field et al., 2018; Naeher et al., 2019). In addition, deposition occurred rapidly with a compacted mass accumulation rate up to ten times greater than the background rate (Hollis et al., 2014; Hines et al., 2019; Naeher et al., 2019). In this study we focus on another primary feature of Waipawa organofacies: the bulk OM is highly enriched in ^{13}C, with a mean $\delta^{13}C_{OM}$ value of -20‰, which is ~7‰ heavier than OM in sediments directly above and below (Schiøler et al., 2010; Hollis et al., 2014; Naeher et al., 2019).

In the absence of evidence for major changes in terrestrial vegetation (Contreras et al., 2014), the lack of isotopically heavy C_4 plants that only evolved in the Neogene (Urban et al., 2010), and no obvious changes in aridity or precipitation (Lomax et al., 2019; Schlanser et al., 2020), we explore the possibility that this ^{13}C enrichment of bulk OM reflects a short-lived drawdown in atmospheric CO_2, reflecting the relationship in carbon isotope discrimination between atmospheric CO_2 and C_3 plant biomass (Cui and Schubert, 2016, 2017, 2018; Schubert and Jahren, 2012, 2018). For this purpose, we analysed the $\delta^{13}C$ values of specific organic fractions (palynodebris) and selected biomarkers from Waipawa organofacies and the "background" bounding facies at two sites (Taylor White and Mid-Waipara sections) to identify the source of ^{13}C enrichment. In addition, we evaluate the roles that lignin degradation (e.g., van Bergen and Poole, 2002) and the sulfurization of OM (e.g., Sinninghe Damsté et al., 1998; Rosenberg et al., 2018) may have played in the ^{13}C enrichment. From these analyses, we estimate the magnitudes of the $\delta^{13}C$ excursion in both primary terrestrial and marine OM and use these values to infer broad changes in the concentration of atmospheric CO_2.

https://doi.org/10.5194/cp-2021-122
Preprint. Discussion started: 17 September 2021

Climate of the Past Discussions

2 Sites and sections studied

This study of Waipawa organofacies includes a compilation of data from ten onshore sections, one onshore and six offshore drillholes from New Zealand and the southwest Pacific (Fig. 2). The sections and site locations are described in Supplement S1 (Fig. S1, Table S1). Waipawa organofacies is most readily identified by $\delta^{13}C_{OM}$ values higher than -24.5‰ (Hollis et al., 2014). Enrichment in total organic carbon (TOC) is also a useful guide although there is wide variation between sections, depending on depositional setting (Hollis et al., 2014). Waipawa organofacies is a defining feature of the Waipawa Formation in the East Coast and Northland basins (Moore, 1988; Isaac et al., 1994; Field et al., 1997) and the Tartan Formation in the Canterbury and Great South basins (Cook et al., 1999; Schiøler et al., 2010). Equivalent facies have also been identified in the Taranaki and West Coast basins (Killops et al., 2000) and the southwest Tasman Sea (Hollis et al., 2014). The background facies in most of the East Coast Basin comprise the underlying Whangai Formation, an organic-poor siliceous to slightly calcareous mudstone, and the overlying Wanstead Formation, an organic-poor non-calcareous to moderately calcareous mudstone (Moore, 1988; Field et al., 1997). In the Marlborough Sub-basin, these two units are replaced by more pelagic facies: siliceous micrites of the Mead Hill Formation and the basal Amuri Limestone (Field et al., 1997; Hollis et al., 2005). In the Great South Basin, the bounding formations are the underlying Wickliffe and overlying Laing Formation (Cook et al., 1999).

This study applies geochemical and palynofacies analyses to rock samples from the Waipawa organofacies and bounding facies in the following stratigraphic sections in northern and eastern and New Zealand: Black's Quarry, Taylor White, Glendhu Rocks (Pahaoa River mouth), Chancet Rocks, Ben More Stream, Mead Stream and mid-Waipara River (Table S1). We combine these new results with published data from the following sections and drillholes: Te Hoe River (Schiøler et al., 2010); Tawanui, Angora Road and mid-Waipara River (Taylor, 2011; Hollis et al., 2014); Taylor White (Naeher et al., 2019); Orui-1A onshore drillhole (Field et al., 2018); Mead Stream (Hollis et al., 2005); Galleon-1 (Schiøler, 2011), Toroa-1, Pakaha-1, Kawau-1A and Hoiho-1C offshore drillholes (Raine et al., 1993; Schiøler et al., 2010), and ODP Site 1172, East Tasman Plateau (Hollis et al., 2014). We also draw on published stable carbon isotope data from spot samples of the Waipawa Formation and bounding formations at Te Weraroa Stream, Angora Stream and Te Puia as well as from Paleocene coaly rock samples (Sykes and Zink, 2012; Sykes et al., 2012).

3 Age control

Hollis et al. (2014) used a combination of nannofossil and dinoflagellate biostratigraphy and limited magnetostratigraphy for the Mead Stream, Angora Road, Tawanui and mid-Waipara River sections and ODP Site 1172 to infer that Waipawa organofacies deposition occurred over ~700 kyrs between ~59.4 and ~58.7 Ma (GTS2012, Gradstein et al., 2012). This age range is consistent with lower resolution age estimates of previous studies (e.g., Schiøler et al., 2010; Crouch et al., 2014; Kulhanek et al., 2015). A new bulk carbonate $\delta^{13}C$ stratigraphy for the interval spanning Waipawa organofacies at Mead Stream allows us to refine this age estimate by correlation with high resolution stable isotope records from North Pacific ODP Site 1209 and South Atlantic ODP Site 1262 (Westerhold et al., 2008, 2011; Littler et al., 2014; Barnet et al., 2019). We use the 2020 Geological Timescale for the Paleogene (Speijer et al., 2020), which incorporates the astronomical age control of Westerhold et al. (2008, 2011, 2017, 2020).

4 Paleontological and geochemical analyses

This study utilises published paleontological and geochemical data from Waipawa Formation sections and sites studied by Schiøler et al. (2010), Sykes et al. (2012), Hollis et al. (2014), Field et al. (2018) and Naeher et al. (2019), unpublished thesis data for the mid-Waipara section (Taylor, 2011), and new analyses from the following sections and sites: Black's Quarry, Taylor White, Glendhu Rocks (Pahaoa River mouth), Mead Stream, Ben More Stream, Chancet Rocks and ODP Site 1172

https://doi.org/10.5194/cp-2021-122
Preprint. Discussion started: 17 September 2021

(Table S1). Homogenised, representative sample aliquots were prepared and palynological and geochemical analyses undertaken using the methods described by Naeher et al. (2019). These included procedures for palynological analysis to determine palynofacies composition (Tables A2 and A3); bulk pyrolysis to quantify OM richness using a Source Rock Analyser (SRA) (Table S2); bulk carbon content and stable isotope analysis using elemental analysis-isotope ratio mass spectrometry (EA-IRMS) (Table S2); solvent extraction and analysis of compound-specific stable carbon isotopes of lipid biomarkers by gas chromatography-combustion-isotope ratio mass spectrometry (GC-C-IRMS) (Table S4); and analysis of kerogen phenol and thiophene concentrations by pyrolysis-gas chromatography-mass spectrometry (Py-GC-MS) (Table S5). Additional procedures employed in this study are described in the following sections.

4.1 Density fractionation

Total organic residues obtained from palynological preparations of eight Waipawa and two Whangai samples from the Taylor White section were solvent-extracted to remove any bitumen present, and then processed by density fractionation with the aim to separate marine and terrestrial constituents of the organic matter. The resulting fractions (3–597 mg) of selected samples were sieved into grain-size fractions <6 µm and ≥6 µm. Both fractions were processed by density separation using sodium polytungstate ($Na_6[H_2W_{12}O_{40}]$; high-purity SPT-0, TC-Tungsten Compounds GmbH, Germany) in deionized water. Five to eight density fractions per grain size fraction were obtained, from <1.2 to >1.5 g cm^{-3}. $\delta^{13}C_{OM}$ values of bulk samples and all density fractions were analysed by EA-IRMS using the instrument conditions as reported in Naeher et al. (2019). These data were compared with palynofacies data obtained from the bulk ≥6 µm fractions using the standard palynological method described in Naeher et al. (2019) (Table S3).

4.2 Solvent extraction, biomarker and carbon stable isotope analyses

To investigate the source and composition of OM, and to help reconstruct depositional and environmental conditions, lipid biomarkers and the carbon isotope composition of the total saturated and aromatic hydrocarbon fractions in solvent extracts (bitumen) from the Taylor White section were previously analysed at Applied Petroleum Technology (APT) in Oslo, Norway, with the methods and data reported by Naeher et al. (2019). Only the carbon isotope values of the total saturated and aromatic fractions (Table S4) and representative mass chromatograms are presented in this paper.

Additional, compound-specific carbon isotope analyses of selected isoprenoids (pristane and phytane), *n*-alkanes (nC_{18}–nC_{33}) (Table S4) and fatty acids (Table S6) were undertaken in the GNS/VUW Organic Geochemistry Laboratory at GNS Science and the Organic Geochemistry Unit (OGU) at the University of Bristol. Samples from the Taylor White section were prepared using the analytical procedures reported in Naeher et al. (2012, 2014) with some modifications. In brief, 7–40 g powdered rock were extracted (4x) with dichloromethane (DCM)/methanol (MeOH) (3:1, v:v) by ultrasonication for 20 min each time. Elemental sulfur was removed by activated copper. The total lipid extracts (TLEs) were divided into saturated and aromatic hydrocarbon, and polar compound fractions via liquid chromatography over silica columns using *n*-hexane, *n*-hexane/DCM (7:3, v:v), and DCM/MeOH (1:1, v:v), respectively. An aliquot of the polar fraction was derivatised with BSTFA [*N,O*-bis(trimethylsilyl)trifluoroacetamide] (Sigma Aldrich) for 1 h at 80°C prior to analysis.

For compound-specific carbon isotope analyses of pristane (Pr), phytane (Ph), and *n*-alkanes (Table S4) we undertook molecular sieving (Dawson et al., 2005; Grice et al., 2008; Aboglila et al., 2010) of free and desulfurized saturated fractions of samples from the Taylor White section. Saturated hydrocarbon fractions dissolved in cyclohexane were added to activated 5Å molecular sieve (Alltech) and heated for 8 h at 80°C. Branched and cyclic compounds were recovered by extraction (5x) with cyclohexane. *N*-alkanes were recovered by dissolution of the sieve with 30% HF, followed by neutralization with saturated $NaHCO_3$ solution. The resulting fractions were analysed using an Isoprime 100 GC-combustion-isotope ratio mass

https://doi.org/10.5194/cp-2021-122
Preprint. Discussion started: 17 September 2021

spectrometer (GC-C-IRMS) system at the University of Bristol, UK. Injection volume was 1 µl onto to a Zebron-I nonpolar column (50 m × 0.32 mm i.d., 0.10 µm film thickness). The GC oven program was: 3 min hold at 70°C, heating to 130 °C at 20°C min^{-1}, then to 300°C at 4°C min^{-1}, and a final hold at 300°C for 25 min. Samples were measured in duplicate and $\delta^{13}C$ values converted to VPDB by bracketing with CO_2 of known $\delta^{13}C$ value. Instrument stability was monitored by regular analysis of an in-house fatty acid methyl ester standard mixture.

The fatty acids from the mid-Waipara section samples were extracted and analysed using a different extraction and separation protocol. Powdered samples were placed in pre-extracted cellulose thimbles and extracted under reflux using a Soxhlet apparatus for 24 h with DCM/MeOH (2:1 v/v) as the organic solvent. The resulting TLEs were separated using an aminopropyl (NH_2) solid phase extraction (SPE) column by elution with DCM/isopropanol (2:1 v/v; neutral fractions), followed by 2% (by volume) acetic acid in diethyl ether (acid fractions). The columns were glass cartridges containing 500 mg of silica-bonded stationary phase, manufactured by Isolute®. Acid fractions were then methylated using BF_3/MeOH complex (14% w/v; 100 µl; 60°C for 30 min). After cooling to room temperature, ~1 ml of double-distilled water was added and then extracted with ~2 ml of DCM. The extracts were passed through a short glass pipette column packed with pre-extracted glass wool and sodium sulphate (Na_2SO_4) (to remove residual water). A further two repeat extractions were performed on each fraction (eluted into the same vial), resulting in a combined extract, which was then dried under N2. The methylated acid fractions were then silylated at 70°C for 1 h.

For compound-specific carbon isotope analyses of the fatty acids (Table S6) GC-C-IRMS was conducted using a Hewlett Packard 6890 gas chromatograph connected to a Thermoquest Finnigan Delta plus XL spectrometer, via a GC III combustion interface (comprising Cu, Pt and Ni wires within a fused alumina reactor at a constant temperature of 940°C). GC conditions were as described above. Duplicate analyses were conducted for each sample, with values mass balance corrected for the addition of a methyl group and reported in standard delta (‰) notation relative to Vienna Pee Dee Bee Belemnite (VPDB). Analytical precision, based on replicate analysis of a standard of mixed fatty acid methyl esters (FAMEs), is < ±0.5‰ (Table S6).

5 Results

5.1 Distinguishing features of Waipawa organofacies

The Waipawa organofacies was defined by Hollis et al. (2014) as a distinctive, organic-rich marine facies in which the organic matter is enriched in ^{13}C. The lithology is typically mudstone, with varying proportions of detrital sand, biogenic silica and glauconite. The additional samples and sites examined in this study confirm that, irrespective of background sediment type, Waipawa organofacies is readily identified by a combination of relatively elevated TOC values, typically >1 wt% up to about 15 wt%, and enriched $\delta^{13}C_{OM}$ values of -24 to -17‰ (Fig. 3, Table S2). There is a positive correlation between TOC and $\delta^{13}C_{OM}$ in all sections examined (Fig. 3), even in sections such as Glendhu Rocks where maximum TOC is low in comparison with other sites (i.e., <0.5 wt%).

5.2 Terrestrial origin of ^{13}C-enriched OM in Waipawa organofacies

5.2.1 Palynofacies evidence

Palynofacies analysis of Waipawa organofacies indicates that, for all sites examined, irrespective of depositional setting, facies or lithology, TOC and ^{13}C enrichment is associated with a dominance of terrestrial OM. In samples where $\delta^{13}C_{OM}$ ranges from -24 to -17‰ (median -20‰), the terrestrial component of palynofacies assemblages is generally greater than 70% (Fig. 4a, Table S2). In most of these samples, the most abundant palynofacies category is degraded woody plant matter (degraded phytoclasts, Fig. 4b).

https://doi.org/10.5194/cp-2021-122
Preprint. Discussion started: 17 September 2021

Climate of the Past Discussions
Open Access
EGU

For all sections studied, total terrestrial palynodebris, total phytoclast and degraded phytoclast abundances have the strongest positive correlations with $\delta^{13}C_{OM}$ of all palynofacies components in bulk samples (Table S2). As most of the terrestrial palynodebris comprises phytoclasts, and high proportions of the phytoclasts in most samples are degraded, we conclude that the positive correlations of total terrestrial palynodebris and phytoclasts with $\delta^{13}C_{OM}$ are heavily influenced by the degraded phytoclast component. To investigate the relationship between ^{13}C enrichment and palynofacies in greater detail, we carried out palynofacies and $\delta^{13}C$ analyses on density-separated fractions of samples from the Taylor White section (Fig. 5, Table S3). In this analysis we differentiate between four lithofacies: (1) Whangai facies (siliceous mudstone underlying Waipawa Formation), (2) organic-rich Waipawa facies (OM-rich; TOC >2 wt%), (3) organic-poor Waipawa facies (OM-poor; <2 wt%), and (4) Wanstead facies (mudstone overlying Waipawa Formation). More detailed descriptions of the lithofacies and stratigraphy are provided by Naeher et al. (2019). In the bulk sediments, the lithofacies are readily distinguished by palynofacies: the two Waipawa facies are dominated by degraded phytoclasts, Whangai facies has a greater proportion of marine components (Fig. 5a), and Wanstead facies has abundant opaque phytoclasts (Naeher et al., 2019). The dominance of opaque phytoclasts in the Wanstead facies is thought to be due to oxidation of all but the most recalcitrant carbon in fully oxygenated depositional conditions (Naeher et al., 2019). Degraded phytoclasts tend to be more abundant in the OM-rich Waipawa facies than in the OM-poor facies. The OM-rich facies also tends to have more positive $\delta^{13}C$ values (~-18‰) than the OM-poor facies (~-22‰), whereas the Whangai and Wanstead facies have $\delta^{13}C$ values of -26 to -27‰ (Fig. 5b). Given the abundance of marine palynodebris in Whangai facies (Fig. 5a), this $\delta^{13}C$ range of -26 to -27‰ provides a baseline for marine OM prior to Waipawa deposition.

Because of the low abundance of OM in Wanstead facies, we were not able to differentiate density fractions for this facies. For the three remaining facies, the marine component [i.e., amorphous organic matter (AOM) + marine palynomorphs (dinoflagellates)] tends to be greater in the light fraction (SG <1.3), and this is especially true of the Whangai and OM-poor Waipawa samples (Fig. 5c, Table S3), which likely explain the generally more depleted $\delta^{13}C_{OM}$ values of these two facies (Fig. 5d). For the heavy fractions (SG >1.3), the terrestrial component is dominant in all three Waipawa and Whangai facies (Fig. 5e). However, degraded phytoclasts are only dominant in the fractions that are most enriched in ^{13}C. For Whangai and some OM-poor Waipawa fractions, non-degraded or opaque phytoclasts (i.e. “Other phytoclasts” in Table S3) dominate the palynofacies assemblage. It is notable that the heavy Whangai fraction, which is dominated by terrestrial palynodebris (Fig. 5e), has an enriched $\delta^{13}C$ value of -21‰ (Fig. 5f). This allows us to benchmark $\delta^{13}C$ values prior to Waipawa deposition at -21‰ for terrestrial OM and -26 to -27‰ for marine OM (Fig. 5b, d). These values are consistent with the findings of Sluijs and Dickens (2012) who derived values of -23.4‰ and -27.3‰ and for terrestrial and marine OM, respectively, for latest Paleocene and early Eocene sediments in the Arctic Ocean. The more positive value for terrestrial OM in the New Zealand records may reflect differences in vegetation between the two regions.

A moderate, positive correlation (R^2=0.56) between degraded phytoclast abundance and $\delta^{13}C$ in the terrestrial-OM dominated heavy fractions (Fig. 5f) indicates that variation in $\delta^{13}C$ in the range of -21 to -17‰ for Waipawa organofacies is primarily a function of the proportion of degraded phytoclasts. Conversely, more depleted $\delta^{13}C$ values in the range of -22 to -25‰ for Waipawa organofacies appear to reflect greater contributions from marine OM sources, especially evident in the light fractions (Figs 5c and d). It is important to note, however, that volumetrically minor contributions of marine OM are present within the heavy and light fractions of both the OM-poor and OM-rich Waipawa organofacies, with volumes reaching 26.7% in the OM-poor samples and 8.3% in the OM-rich samples (Table S3). Thus, despite positive correlations between $\delta^{13}C$ and degraded phytoclast abundance (Fig. 5b, d and f), the subordinate contributions of marine OM will also have an influence on the $\delta^{13}C$ values of bulk samples that cannot be readily eliminated.

https://doi.org/10.5194/cp-2021-122
Preprint. Discussion started: 17 September 2021


Climate of the Past Discussions
Open Access
EGU

5.2.2 Geochemical evidence

Various geochemical indicators, such as higher plant biomarkers of mainly angiosperm origin, also point to the dominance of terrestrial OM in Waipawa organofacies in the Taylor White section (Naeher et al., 2019). The Waipawa facies is enriched in pristane, phytane and odd carbon-numbered high molecular weight (HMW; C_{27}–C_{31}) *n*-alkanes relative to the OM-poor Waipawa and Whangai facies (Fig. 6a). The prevalence of HMW *n*-alkanes with odd-over-even predominance is consistent with a higher-plant-dominated organofacies (Peters et al., 2005). Although pristane and phytane are typically derived from algal chlorophyll (phytol component) in marine sediments, the dominance of terrigenous OM in Waipawa organofacies suggests that a proportion of these compounds is derived from leaf chlorophyll. The same suite of compounds occurs in the OM-poor Waipawa organofacies (Fig. 6b) but the HMW *n*-alkanes are not as prominent as in the OM-rich facies, with greater proportions of low and medium molecular weight (LMW, C_{17}–C_{19}; MMW, C_{21}–C_{25}) *n*-alkanes indicating a greater marine contribution. While this facies still has a high abundance of terrestrial OM, an overall lower abundance of degraded phytoclasts may explain the relatively depleted $\delta^{13}C$ values compared to those of the OM-rich Waipawa facies. The same suite of compounds is also present in Whangai facies (Fig. 6c) but with a greater abundance of LMW *n*-alkanes signalling an even greater marine contribution, as indicated by moderate–high proportions of marine palynodebris (22.3–85.9%, Table S2). Nonetheless, abundant HMW *n*-alkanes in all three facies indicate a persistent terrestrial contribution, although the chlorophyll-derived pristane and phytane are likely to be a mixture of both terrestrial and marine inputs. This is supported by the enrichment of some specific marine biomarkers, notably C_{30} steranes, which indicate that Waipawa deposition was also associated with an increased abundance of specific groups of marine algae in most settings (Murray et al., 1994; Killops et al., 2000; Hollis et al., 2014; Naeher et al. 2019).

The variable contribution of terrestrial OM to both the Waipawa and Whangai organofacies in the Taylor White section and its influence on their respective $\delta^{13}C_{OM}$ values is further reflected by the abundance of lignin-derived phenols within their kerogen fraction (Table S5). Naeher et al. (2019) first reported a strong, positive correlation (R^2=0.83) of the phenols/naphthalene ratio with increasing TOC from the Whangai facies to the OM-poor and OM-rich Waipawa facies, highlighting the dominant influence of transported, higher plant-derived woody OM (i.e., phytoclasts) on the organic enrichment of Waipawa organofacies. In the present study, this relationship is extended to the enrichment in ^{13}C, with a strong, linear correlation (R^2 = 0.79) displayed between the phenols/naphthalene ratio and $\delta^{13}C_{OM}$ (Fig. 7a). This correlation confirms that $\delta^{13}C_{OM}$ increases to a maximum value of -17‰ as the abundance of woody material increases in the sediment.

5.3 Possible autogenic causes of ^{13}C enrichment

Having established that the ^{13}C-enrichment appears to be linked primarily to the dominance of terrestrial-derived degraded phytoclasts in the Waipawa OM (Fig. 5), we now consider how and to what extent OM degradation or indeed preservation processes within the broader depositional environment might account for the ^{13}C-enrichment. Only by accounting for potential processes of ^{13}C-enrichment during OM transportation, deposition and early diagenesis it is possible to identify any residual enrichment that may be related to a drawdown in atmospheric CO_2 levels.

5.3.1 Sulfurization

The preservation of carbohydrates through sulfurization is an established mechanism for ^{13}C enrichment in fossil organic matter (Sinninghe Damsté et al., 1998; van Kaam-Peters et al., 1998) and was previously suggested for the Waipawa organofacies by Hollis et al. (2014). Naeher et al. (2019) reported a strong, positive correlation (R^2 = 0.80) between the sulfur-containing thiophenes and HI for Waipawa and other facies in the Taylor White section. However, whilst this correlation supports the concept of increased preservation of the bulk OM assemblage through sulfurization, the present study of the Taylor White section has revealed only a weak correlation (R^2 = 0.20) between thiophenes and $\delta^{13}C_{OM}$ for the

https://doi.org/10.5194/cp-2021-122
Preprint. Discussion started: 17 September 2021

Waipawa and Whangai samples (Fig. 7b). If only the Waipawa organofacies samples are considered and the two outlier samples TW-15 and -17 from just above the transition zone at the base of the main Waipawa interval are excluded (Naeher et al., 2019, fig. 2), the correlation coefficient between thiophenes/naphthalene and $\delta^{13}C_{OM}$ increases slightly ($R^2 = 0.37$). This suggests that the preservation of carbohydrates by sulfurization is potentially at best only a secondary influence on ^{13}C enrichment within the Waipawa organofacies. Indeed, the opposing process of tissue degradation appears to have been far more influential given the strong correlation between degraded phytoclast abundance and $\delta^{13}C_{OM}$ (Fig. 5).

5.3.2 Lignin degradation

The main macromolecular components of woody plants are cellulose and lignin. These components have different susceptibilities to degradation, and this has been shown to alter the $\delta^{13}C$ of woody plant matter (Gröcke et al., 1999; Schleser et al., 1999; Schweizer et al., 1999; van Bergen and Poole, 2002; Fernandez et al., 2003). According to these studies, $\delta^{13}C_{OM}$ decreases during early diagenesis due to the rapid degradation of cellulose and the consequent increase in the relative concentration of the more recalcitrant lignin. Eventually, however, the lignin begins to degrade too, and this can lead to an increase in $\delta^{13}C_{OM}$ values (Hedges et al., 1985; Gröcke, 1998; Gröcke et al., 1999; van Bergen and Poole, 2002). Van Bergen and Poole (2002, fig. 1) suggested enrichment in $\delta^{13}C$ of up to about 7–8‰ can occur in lignin as a result of demethylation and dehydroxylation reactions. This seems a plausible cause for the relationship described above for the heavy fraction (SG <1.3) of the OM-rich Waipawa facies samples from the Taylor White section (Fig. 5f) in which an increase in the proportion of degraded phytoclasts from 20 to 90% corresponds to a ~5‰ increase in $\delta^{13}C$. The heavy fraction results provide the best evidence of the effects of phytoclast degradation on $\delta^{13}C$ values because this fraction generally contains less marine organic matter (Figs 5c, 5e).

If lignin degradation is the main cause of ^{13}C enrichment within the Waipawa organofacies, we would expect the aromatic hydrocarbon fraction to be more strongly enriched than the saturated fraction, and this is indeed what we observe for Waipawa samples from Taylor White and other sections (Fig. 8a). For the 16 OM-rich Waipawa samples with both $\delta^{13}C_{Sat}$ and $\delta^{13}C_{Aro}$ values in Table S4, the aromatic fraction is enriched in ^{13}C relative to the saturated fraction in all cases by 1.5 to 4.8‰, averaging 3.3‰.

The relationship between $\delta^{13}C_{Sat}$ and $\delta^{13}C_{Aro}$ for different types of organic matter can be expressed by the canonical variable (CV) of Sofer (1984; see also Holman and Grice, 2018), derived from the following equation:

$$CV = -2.53\ \delta^{13}C_{Sat} + 2.22\ \delta^{13}C_{Aro} - 11.65$$

On a cross-plot of $\delta^{13}C_{Sat}$ and $\delta^{13}C_{Aro}$ (Fig. 8a), CV values essentially represent the perpendicular distance of samples from the so-called Sofer line, which has a CV value of 0.47 (Fig. 8b). Samples plotting above the Sofer line (i.e., CV >0.47) typically contain OM primarily of terrestrial origin and have aromatic hydrocarbon fractions more enriched in ^{13}C than their saturated fractions, and vice versa for samples with CV <0.47 typically comprising primarily marine OM.

Most Waipawa organofacies samples from the Taylor White and several other sections plot within the terrestrial field (Fig. 8a). The only Waipawa sample from Taylor White that plots in the marine field with the Whangai and Wanstead samples is sample TW-19, which potentially contains a greater content of marine OM than is indicated by its palynofacies results (Table S2). Some Waipawa samples from Taylor White, including most of the OM-poor samples, have CV values between 0.47 and 5 (Fig. 8b). This range also includes a selection of New Zealand Paleocene coaly rocks comprising solely terrestrial OM deposited essentially *in situ* and which can be reasonably inferred to be relatively well preserved given the generally reducing conditions within peat deposits. In contrast, many of the OM-rich Waipawa samples from Taylor White have exceptionally high CV values between 5 and 8 (Fig. 8b), indicating particularly strong ^{13}C enrichment of the aromatic

https://doi.org/10.5194/cp-2021-122
Preprint. Discussion started: 17 September 2021


Climate of the Past Discussions
Open Access
EGU

fractions, potentially due to lignin degradation. It could be argued, therefore, that CV values primarily represent the degree of wood tissue degradation within the Waipawa organofacies, but this would ignore the subordinate contributions of marine OM in many of the samples, which would tend to reduce CV values despite high proportions of degraded phytoclasts. As noted in Section 3.2.1., the OM-poor Waipawa samples tend to contain significant proportions of marine OM in their light fractions (SG <1.3, Fig. 5c). Similarly, the very OM-rich Waipawa samples from the Black's Quarry (E012, E013) and Te Puia (E113) sections, with highly ^{13}C-enriched aromatic and saturates fractions, have low CV values of -0.47 and -0.79 within the marine OM field (Fig. 8a). These samples do not have palynofacies data, but their solvent extracts are rich in C_{30} steranes indicative of a significant marine algal component (Sykes and Zink, 2012), while some OM-rich Waipawa samples in the Taylor White section, including TW-2, which also has a low CV value (Fig. 8), are also enriched in C_{30} steranes (Naeher et al., 2019). This mixing of terrestrial and marine OM, which is evident in most Waipawa samples to varying degrees, hinders the use of bulk $\delta^{13}C$ parameters (e.g., $\delta^{13}C_{OM}$, $\delta^{13}C_{Sat}$, $\delta^{13}C_{Aro}$ and CV) in apportioning ^{13}C enrichment to specific autogenic processes, such as sulfurization and lignin degradation. Moreover, it adds to the difficulty in using these bulk parameters to confidently identify any residual ^{13}C enrichment related to drawdown of atmospheric CO_2.

5.4 ^{13}C enrichment attributable to drawdown of atmospheric CO_2

To circumvent the complications of lignin degradation, and source mixing on the $\delta^{13}C$ values of the bulk OM and the saturated and aromatic hydrocarbon fractions, we now focus on compound-specific carbon isotope analysis of sediments from the Taylor White (Fig. 9a–b) and mid-Waipara sections (Fig. 9c). In the Taylor White section, we analysed pristane, phytane and C_{18}–C_{33} *n*-alkanes ($\delta^{13}C_{Pr}$, $\delta^{13}C_{Ph}$, $\delta^{13}C_{18}$, etc.; Table S4). In the mid-Waipara section, we analysed the C_{16}–C_{32} *n*-alkanoic or fatty acids (Table S6) because the OM in this section was particularly immature and thus, there were insufficient concentrations of *n*-alkanes. For most compounds in both sections, irrespective of whether they are derived from terrestrial, aquatic or marine sources, the $\delta^{13}C$ trends parallel that of the bulk OM to a greater or lesser extent (Fig. 9) and exhibit a significant positive correlation with $\delta^{13}C_{OM}$ (Fig. 10). Particularly strong correlations with $\delta^{13}C_{OM}$ are noted for pristane ($R^2 = 0.93$) and the MMW *n*-alkanes (exemplified by $\delta^{13}C_{23}$, $R^2 = 0.91$) at Taylor White (Fig. 10a) and with the $C_{28–30}$ HMW fatty acids ($R^2 = 0.86$) at mid-Waipara (Fig. 10b). Despite parallel trends, the magnitudes of the positive carbon isotope excursion (+CIE) differ considerably (Fig. 11a, b). Of the compound-specific components, phytane exhibits the largest +CIE (~7‰), followed by pristane and the fatty acids (~4‰), the LMW and MMW *n*-alkanes (2–3‰) and then the HMW *n*-alkanes (~1‰) (Fig. 11c, d).

Variations in the magnitude of the $\delta^{13}C$ excursions amongst different compound classes are commonly due to mixing of OM sources, as discussed above for bulk fractions, or due to different isotopic sensitivities to environmental change in the source organisms (Pancost et al., 1999; Schouten et al., 2007). The strong correlation between the carbon isotope compositions or pristane and phytane with $\delta^{13}C_{OM}$ (Fig. 10a) suggests that they derive from a mixture of terrestrial and aquatic sources in the Taylor White section, with the terrestrial source dominant in Waipawa organofacies. Thus, the pristane CIE implies that the primary terrestrial substrate is enriched in ^{13}C by ~4‰. The greater CIE for phytane (Fig. 11c) suggests an additional unidentified source of enriched carbon.

The LMW and MMW *n*-alkanes and fatty acids, which are thought to be derived mainly from aquatic sources, exhibit positive $\delta^{13}C$ shifts of about 2–4‰ in the Waipawa organofacies relative to the respective mean values in the underlying facies (Fig. 11c, d). These shifts may reflect a change in substrate $\delta^{13}C$ or secondary processes that enhance carbon isotope discrimination during photosynthesis such as a decline in atmospheric CO_2 concentration or an increase in plant growth rates (Bidigare et al., 1997).

https://doi.org/10.5194/cp-2021-122
Preprint. Discussion started: 17 September 2021


Climate of the Past Discussions

The $\delta^{13}C$ values of primarily higher plant derived biomarkers, HMW *n*-alkanes at Taylor White and HMW fatty acids at mid-Waipawa (Fig. 11c, d), exhibit different degrees of $\delta^{13}C$ enrichment. The HMW fatty acids exhibit a similar level of enrichment as the aquatic biomarkers (~3–4‰), whereas the HMW *n*-alkanes exhibit the lowest level of enrichment (~1‰) for all compounds. Enrichment of ~1‰ is also observed in deep-sea foraminiferal carbonate in the late Paleocene (Fig. 1). However, because the HMW fatty acids exhibit a significantly larger carbon isotopic enrichment, it is possible that the HMW *n*-alkanes at Taylor White derive from not multiple terrestrial sources. It is possible that a combination of contemporaneous and older reworked sources, might dampen the signal from contemporaneous higher plants (e.g., Carmichael et al., 2017).

We find support for this possibility in additional compound-specific $\delta^{13}C$ analyses undertaken from OM-rich Waipawa organofacies at Angora Road and Mead Stream (Fig. 12). At these sites, Waipawa organofacies has similar $\delta^{13}C$ values for phytane, pristane, LMW and MMW *n*-alkanes as at Taylor White. However, in contrast to the weakly enriched HMW *n*-alkane values at Taylor White, the HMW *n*-alkanes at Angora Stream and Mead Stream are as enriched as the other of the *n*-alkanes at these sites. This suggests that the depleted HMW values at Taylor White could well be due to mixing with an older source and the contemporaneous higher plant input is better represented by values of ~-27.5‰ recorded at Mead and Angora. This implies an excursion of ~2.5‰, which is consistent with the HMW fatty acids at MW.

In summary, most of the organic compounds we have analysed are enriched in ^{13}C in the OM-rich Waipawa organofacies relative to bounding facies. The evidence indicates that a significant excursion of at least 2.5‰ for compounds derived primarily from aquatic OM, which signals a pronounced if short-lived perturbation in the global carbon cycle. Crucially, we have demonstrated that the $\delta^{13}C$ trends in all aquatic and terrestrial biomarkers parallel the trends in bulk organic matter in the Taylor White and mid-Waipara sections (Fig. 10). This implies that the primary influence on $\delta^{13}C_{OM}$, the proportion of degraded woody plant matter, is modulated by the same carbon cycle changes that cause the variation in $\delta^{13}C$ in both aquatic and terrestrial biomarkers. For practical purposes, it also implies that we can utilise variations in $\delta^{13}C_{OM}$ to correlate Waipawa organofacies successions and make comparisons with global climate records.

6 Discussion

6.1 Correlation and age of Waipawa organofacies deposition

We can establish the timing of Waipawa organofacies deposition by correlating the Paleocene bulk carbonate $\delta^{13}C$ record at Mead Stream (Fig. 13a; Supplementary Material S2) with the high-resolution bulk carbonate and benthic foraminifera $\delta^{13}C$ records from ODP sites 1209 and 1262 (Barnet et al., 2019; Westerhold et al., 2020). Waipawa deposition coincides with the onset of the Paleocene carbon isotope maximum (PCIM; Fig. 1), a ~2 million-year episode in which $\delta^{13}C$ values for marine carbonate reach their Cenozoic maximum. Waipawa deposition spans the first 800 kyr of this event, extending from 59.2 to 58.4 Ma. This age range improves on previous estimates (Crouch et al., 2014; Hollis et al, 2014; Kulhanek et al., 2015) and is consistent with a new age estimate of 57.5 ± 3.5 Ma derived from Re-Os geochronology (Rotich et al., 2020). Carbonate $\delta^{13}C$ increases by 0.5–0.7‰ over this first part of the PCIM, with a larger excursion (0.7‰) recorded at South Atlantic Site 1262 than at North Pacific Site 1209 (0.5‰). This excursion accounts for only a small fraction of the Waipawa organofacies excursion of 2.5‰.

Waipawa deposition also occurs within a Paleogene maximum in marine carbonate $\delta^{18}O$, which extends from 59.6 to 58.2 Ma (Fig. 1, 13b). We refer to this interval as the **Paleocene oxygen isotope maximum (POIM)** here. Although this interval signals cooling of bottom waters, it also includes a short-lived, putative warming event referred to as the early late Paleocene event or ELPE (Fig. 13a, b). Waipawa deposition appears to occur directly after this event, which is identified by a distinct

https://doi.org/10.5194/cp-2021-122
Preprint. Discussion started: 17 September 2021

negative excursion in carbonate $\delta^{13}C$ at Mead Stream (Fig. 13a). In contrast to Eocene hyperthermals that are associated with marl-rich intervals in the micritic limestone succession (Hollis et al, 2005; Slotnick et al., 2012), no obvious changes in lithology are associated with the ELPE at Mead Stream.

Waipawa deposition also coincides with a marked decrease in the coarse fraction in foraminiferal residues from sites 1209 and 1262 (Fig. 1, 13b). This represents a marked decrease in the abundance of planktic foraminifera and is attributed to carbonate dissolution (Littler et al., 2014). Although short-lived dissolution episodes have been linked to the PETM and other early Eocene hyperthermals (Zachos et al, 2005; Alexander et al., 2015), the longer duration of this episode and its association with positive shifts in both $\delta^{13}C$ and $\delta^{18}O$ suggest a link to climatic cooling and carbon burial as outlined by Hilting et al. (2008).

6.2 Waipawa organofacies associated with climatic cooling and CO_2 drawdown

Positive correlations between $\delta^{13}C_{OM}$ and the TEX_{86} SST proxy at mid-Waipara River and ODP Site 1172 (Fig. S8) indicate that Waipawa deposition is associated with significant cooling of coastal waters (Hollis et al., 2014; Bijl et al., 2021). Cooling on land is also indicated by temperature reconstructions based on pollen assemblages at Site 1172 (Contreras et al., 2014). Correlation with the POIM in the deep-sea isotope record (Westerhold et al., 2011; Littler et al., 2014, Barnet et al., 2019) further suggests that the positive $\delta^{13}C$ excursion in Waipawa organofacies (Fig. 13c–f) is linked in some way to climatic cooling. Although the large 8‰ excursion in bulk OM (Fig. 13c) is inferred to be partly a result of lignin degradation, excursions of 2.5‰ in HMW *n*-alkanes and fatty acids (Fig. 13d) and 4‰ in MMW and LMW *n*-alkanes and fatty acids, as well as in pristane (Fig. 13e, f) are clear indications of major perturbations in the terrestrial and marine environments. Such carbon isotopic shifts can be caused by a range of environmental factors, but a correlation with climatic cooling implies that a portion of the carbon shift is caused by a decline in atmospheric CO_2. A decline in CO_2 will result in ^{13}C enrichment in the biomass of algae (Freeman and Hayes, 1992) as well as in higher plants (Cui and Schubert, 2016; Cui and Schubert, 2017; Cui and Schubert, 2018; Schubert and Jahren, 2012; Schubert and Jahren, 2018).

We refrain from estimating a CO_2 change due to the complex mixing of OM sources. However, the deep-sea benthic $\delta^{18}O$ record indicates that deep sea temperatures decreased by 1°C in the POIM (Barnet et al., 2019), which is consistent with a modest (20–30%) decline in CO_2, assuming a climate sensitivity of 3°C. Locally, a much more pronounced cooling is recorded: by 6°C at Site 1172 and by 4°C at mid-Waipara (Fig. 13b), but these values may reflect localised phenomena such as upwelling of Antarctic deep water (Hollis et al. 2014).

6.3 New insights into the depositional setting of Waipawa organofacies

Waipawa organofacies is widely distributed in the southwest Pacific (Fig 1), occurring in most of New Zealand's sedimentary basins as well as the East Tasman Plateau (Hollis et al., 2014). It is inferred to have been deposited at a range of paleodepths, from inner shelf to mid-slope (Moore, 1988; Schiøler et al., 2010; Naeher et al., 2019), and within a narrow time window of ≤1 Myr in the early late Paleocene (~59 Ma; Hollis et al., 2014). Previously, Waipawa organofacies was thought to have been deposited during a regression or lowstand following a base level fall (Schiøler et al., 2010; Hollis et al., 2014). However, benthic foraminiferal assemblages in the Taylor White section are interpreted as indicating a general deepening or transgressive trend from the underlying Whangai and into the overlying Wanstead Formation (Naeher et al., 2019). This suggests an alternative interpretation of the palynofacies assemblages within the Waipawa organofacies is required. If we examine how palynofacies assemblages vary in relation to proximity to paleo-shoreline for our studied sections (Fig. 14), we find that a conventional distribution is evident for the underlying facies, i.e. Whangai or Wickliffe Formations (Fig. 14a). Terrestrial components (i.e., phytoclasts + terrestrial palynomorphs) tend to decrease whereas marine

https://doi.org/10.5194/cp-2021-122
Preprint. Discussion started: 17 September 2021


Climate of the Past Discussions

elements (amorphous organic matter + marine palynomorphs) increase with water depth and hence with distance from shore. However, the relationship is reversed for Waipawa organofacies: terrestrial components increase whereas marine components decrease with water depth and distance from shore (Fig. 14b). Degraded phytoclasts, in particular, exhibit a pronounced increase in abundance in the deeper and more distal sections. This distribution of terrestrial OM is supported by biomarkers, which show terrestrial influence is strongest in the sections with thickest accumulations of Waipawa sediments (e.g., Taylor White and Orui-1A) and weakest in both more proximal (Te Hoe) and more distal (Mead, Ben More) settings (Fig. 15, Fig. S2).

We interpret this to indicate that Waipawa organofacies is the result of a rapid influx of terrestrial OM into the marine environment. Corroborating evidence for a marked increase in terrestrial runoff at this time has recently been reported in a study of biomarkers and dinoflagellate paleoecology from ODP Site 1172 (Bijl et al. 2021). The foraminiferal data (Naeher et al., 2019) suggest that this runoff event occurred while basins were progressively deepening, which is consistent with long-term passive-margin subsidence throughout New Zealand (King et al., 1999). This discovery resolves a long-standing enigma in New Zealand geology. In all of the sedimentary basins to the east of New Zealand, a transition from siliciclastic to hemipelagic sedimentation occurs in the late Paleocene. If Waipawa organofacies is present, this facies transition occurs immediately above (e.g. Whangai–Waipawa–Wanstead transition in the East Coast Basin; Field et al., 1997). It difficult to develop a credible depositional model in which a nearshore Waipawa facies was sandwiched between two bathyal units, the overlying one being deeper bathyal than the underlying one.

6.4 Global correlations and drivers of Waipawa organofacies

When correlated to deep sea benthic isotope records (Westerhold et al., 2011, 2020; Littler et al., 2014; Barnet et al., 2019), Waipawa organofacies deposition is found to coincide with a minimum in deep-sea temperatures and the onset of the 2.2 Myr-long PCIM (Fig. 1). Several factors have been implicated in the long-term trends in Paleocene temperature and carbon cycling. Cooling from late early to middle Paleocene (63–60 Ma) followed by warming in the late Paleocene (58–56 Ma) has been linked to global trends in volcanism (Westerhold et al., 2011), continental rifting (Brune et al., 2017), and tectonism (Beck et al., 1995; Kurtz et al., 2003; Rotich et al., 2020). Based on the decoupling of carbon and sulfur cycles, Kurtz et al. (2003) argued that the PCIM records enhanced accumulation of terrestrial carbon as a result of tectonic uplift. They point to the vast coal deposits of the Powder River Basin, which represent the swamps that replaced North America's epeiric seas during the Laramide orogeny. Our observation that the OM in the Waipawa organofacies is also terrestrial adds another, albeit offshore, sink for terrestrial organic carbon at this time. Hilting et al. (2008) also interpret the PCIM to be a time of enhanced terrestrial carbon burial and reduced CO_2 levels. Terrestrial carbon burial is modelled to have reduced dissolved inorganic carbon (DIC) in the global ocean (Hilting et al., 2008). This is consistent with our correlation of Waipawa organofacies with an interval of carbonate dissolution during the initial part of the PCIM (Fig. 1). During the second part of the PCIM, carbonate accumulation recovered at the same time as deep-sea temperatures begin to increase (Barnet et al., 2019), suggesting that a new source of carbon offset the effects of carbon burial, such as the CO_2 outgassing from the second phase of North Atlantic Igneous Province (NAIP) volcanism (Westerhold et al., 2011). Recently, Rotich et al. (2020) showed that Waipawa deposition coincides with a Paleocene minimum for radiogenic osmium (Os). They suggested that this reflected the broad climate trend through the Paleocene, with reduced radiogenic Os produced by continental weathering during the relatively cool mid-Paleocene (i.e. the POIM).

Terrestrial organic $\delta^{13}C$ values in the same range (-24 to -17 ‰) as those reported for Waipawa organofacies have been reported from nonmarine Paleocene sections in China (Clyde et al., 2008) and Argentina (Hyland et al., 2015). In the middle Paleocene Chijiang Basin section in China, a positive $\delta^{13}C_{OM}$ excursion occurs from background of values of -24 to -22 ‰ to

https://doi.org/10.5194/cp-2021-122
Preprint. Discussion started: 17 September 2021

-17 ‰ (Clyde et al., 2008). This demonstrates that similar processes may have affected terrestrial plant matter in regions beyond the southwest Pacific, i.e. lignin degradation and CO_2-controlled carbon fractionation. However, magnetostratigraphy for this section indicates that the excursion predates the Waipawa event by ~1 Ma.

In the Salto Basin section in Argentina, a middle–late Paleocene section comprises two cycles in which $\delta^{13}C_{OM}$ ranges from depleted values of -26 to -25‰ to enriched values of -21‰, again a shift similar to that recorded by Mid-Waipara HMW fatty acids. The enriched values are linked to proxies for lower temperature and lower precipitation (Hyland et al., 2015). A 30 m-thick interval with enriched $\delta^{13}C_{OM}$ values at the base of the late Paleocene (lower Chron 26n) is very sparsely sampled and may correlate with the Waipawa event. It is sandwiched between two intervals with more depleted $\delta^{13}C_{OM}$ values that are correlated with a two-phase early late Paleocene event (ELPE – Petrizzo, 2005; Bernaola et al., 2007).

Some have argued that the ELPE is a hyperthermal (Bernaola et al., 2007). However, it lacks two distinctive features of hyperthermals: a negative excursion in $\delta^{13}C$ (in fact $\delta^{13}C$ increases) and clear evidence for warming. Possible evidence for warming is seen at ODP site 1262 (Littler et al., 2014; Barnet et al., 2019), where individual samples record depleted $\delta^{18}O$ values. However, these samples are anomalies against a background of relatively enriched values and may be more plausibly explained by downslope transport of individual benthic foraminifera. Moreover, a burrowed horizon near the base of the ELPE at Site 1262 (1262B-18H-4, 97–127 cm) suggests the presence of an unconformity and, therefore, an incomplete record.

The high-resolution records from sites 1209 and 1262 indicate that the ELPE marks a significant turning point in Paleocene climate and carbon cycling: the termination of a long-term (4 Myr) cooling trend followed by a prolonged period of carbon burial, the PCIM (Kurtz et al., 2003). Significantly, benthic foraminiferal $\delta^{18}O$ and $\delta^{13}C$ trends are coupled from 63 to 59 Ma, with positive shifts in both parameters suggesting that cooling was associated with declining atmospheric CO_2 (Fig. 1). From 59 to 58 Ma, the trends are not coupled: $\delta^{13}C$ continues to increase while $\delta^{18}O$ either decreases or remains stable. From 58 Ma to at least the early Eocene, the records are once more coupled. Evidence from neodymium isotopes indicates that deep-water exchange between the North and South Atlantic intensified at 59 Ma due to the deepening of the central Atlantic Rio Grande Rise (Batenburg et al., 2018). The latter authors argue that this intensification of overturning may have triggered the Paleocene–Eocene warming trend. However, there was no deep-water connection with the much larger Pacific Ocean basin at this time (Thomas et al., 2014), so it is uncertain how this change in the Atlantic would have triggered a global response.

7 Conclusions

Correlation of Paleocene sedimentary successions in the Southwest Pacific with deep-sea stable isotope records has revealed that deposition of Waipawa organofacies occurred over a period of ~800 kyrs within an episode of global cooling and increased carbon burial between 60 and 58 Ma (Figs. 1, 13. The sequence of events that led to deposition of Waipawa organofacies is highly unusual, if not unique, in the geological record. The organic-rich nature of the marine mud facies is due mainly to massive input of degraded woody plant matter. Both this plant matter and a subordinate amount of marine algal material are collectively enriched in ^{13}C by as much as ~7–10‰. This is partly a result of degradation processes during OM transportation and deposition, and probably also local environmental factors. However, a residual excursion of ~2.5‰ is consistent with the long-term positive $\delta^{13}C$ excursion that defines PCIM. Episodes of carbon burial and climatic cooling are common in the geological record, but this event appears unique in resulting in the regionally widespread and rapid deposition of degraded terrestrial plant matter. We postulate a scenario in which four independent processes are at play:

https://doi.org/10.5194/cp-2021-122
Preprint. Discussion started: 17 September 2021


Climate of the Past Discussions
Open Access
EGU

i) *A pause in North Atlantic volcanism*. Climate cooled in the middle Paleocene as the first phase of NAIP volcanism subsided and volcanic CO_2 emissions decreased. Climatic cooling is likely to have increased the storage of carbon as biogenic methane in continental shelves (Dickens, 2003) and in high-latitude permafrost (DeConto et al., 2012). This would have led to a positive feedback in which carbon burial caused further lowering of atmospheric CO_2 and further cooling. Climate then warmed through the later Paleocene and Eocene as the second phase of NAIP volcanism ramped up.

ii) *North American tectonism*. Between these two volcanic CO_2-modulated climate shifts, the Laramide uplift event is thought to have turned the vast epeiric seas in North America into peat swamps, forming a further large carbon sink (Kurtz et al., 2003) and leading to further CO_2 drawdown, cooling and carbonate dissolution in the deep sea (Hilting et al., 2008). Global sea level records indicate a significant fall in sea level occurred at this time, namely the Th2 event of Hardenbol et al. (1998) and the Pa2b event of Kominz et al. (2008). Harris et al. (2010) infer that this event corresponds to a glacioeustatic fall in sea level of ~15 m.

iii) *Southwest Pacific tectonism*. In the context of long-term passive margin subsidence and the opening of the Tasman Sea, rapid basinal deepening occurred through much of the Southwest Pacific in the late Paleocene as evidenced by the transition from siliciclastic to hemipelagic to pelagic carbonate facies in the Great South, Canterbury, East Coast and North Slope basins east of New Zealand (Field et al., 1989, 1997; Cook et al., 1993; Isaac et al., 1994; King et al., 1999). Foraminiferal assemblages in the Taylor White succession confirm that this transgression progresses through the Waipawa Formation and into overlying Wanstead Formation (Naeher et al., 2019). A similar geological history is inferred for the Tasmanian margin where a major runoff event is linked to Waipawa deposition (Hill and Exon, 2004; Bijl et al., 2021). Therefore, the only plausible explanation for a rapid influx of terrestrial plant matter is one or more eustatic falls in sea level, eroding coastal vegetation and flushing the debris into offshore basins.

iv) *Orbital forcing*. The Paleocene includes five 2.4-Myr eccentricity cycles, each of which comprise six 405-kyr cycles (Barnet et al., 2019). Waipawa organofacies deposition occurred during a ~1-Myr decline in eccentricity forcing with the maximum coinciding with the ELPE and the minimum coinciding with the "*" event (Fig. 1). Three of the other eccentricity minima occur at times that the NAIP was active, whereas the first occurred at ~64.5 Ma and corresponds with a pronounced regional cooling event (Taylor et al, 2018).

All four processes appear to have had a role in creating Waipawa organofacies. A relatively warm climate from late early to middle Paleocene allowed expansion of terrestrial vegetation despite a regional transgression. Cessation of CO_2 emissions from NAIP volcanism combined with an eccentricity minimum to cause rapid cooling in the early late Paleocene. Lower CO_2 levels may also be attributed to increased carbon burial in North America swamps coupled with sequestration of biogenic methane in continental shelves and high-latitude permafrost as positive feedbacks. Growth of ephemeral ice sheets then caused sea levels to fall and coastal erosion, leading to rapid transportation and deposition of terrestrial plant matter. It is likely that the interplay of eccentricity-modulated climate cycles and basinal subsidence led to pulses of erosion, deposition and redeposition, which provides a mechanism for seafloor degradation of woody plant matter to occur prior to remobilisation and redeposition. A similar scenario during late Miocene lowstands led to large accumulations of terrestrial OM in the deep-water Kutei Basin in East Kalimantan (Saller et al., 2006).

It now seems likely that the variation in TOC and $\delta^{13}C_{OM}$ seen in expanded records of Waipawa organofacies such as the Taylor White section can be correlated to similar scales of variation in the high-resolution benthic isotope records. Confirmation of this would require more closely spaced sampling than has been possible in this study, ideally as part of a stratigraphic drilling project.

https://doi.org/10.5194/cp-2021-122
Preprint. Discussion started: 17 September 2021

Previous studies of past greenhouse climates of the early Paleogene have identified short-lived global warming events, termed hyperthermals, that have been the subject of numerous studies because of the insights they offer for understanding projected global warming scenarios (Zachos et al., 2008; Sexton et al., 2011; Westerhold et al., 2018; Barnet et al., 2019). Within the same time interval, we have identified a similarly short-lived cooling event, which we term a hypothermal, that has potential to offer insights into how the planet may recover from global warming.

Acknowledgments

Funding for this study came from the Ministry of Business, Innovation and Employment (MBIE), New Zealand, as part of the GNS Science-led programme "Understanding petroleum source rocks, fluids, and plumbing systems in New Zealand basins: a critical basis for future oil and gas discoveries" (Contract C05X1507). Initial work was supported by the New Zealand Marsden Fund. We thank R. McDonnell, S. Bermudez and H. Gard for crushing and powdering rocks, R. Tremain for preparing samples for palynological analyses, and A. Phillips, A. Immers, J. Cooper and J. Fitzgerald for bulk organic matter carbon isotope analyses. Applied Petroleum Technology (Norway) is thanked for lipid biomarker analyses. The International Ocean Discovery Programme provided samples from ODP site 1172. Kate Littler, James Barnet, Thomas Westerhold, Jerry Dickens, Peter Bijl and Matt Huber are thanked for sharing data and providing valuable insights and stimulating discussion in the course of this work.

Author Contributions

C.J.H., S.N., C.D.C., and R.S. designed, directed and led the study. S.N., G.T.V., C.D.C., J.D., X.L., B.D.A.N. and K.W.R.T. acquired and analysed the data. C.J.H., S.N., C.D.C., B.D.A.N., R.D.P. and R.S. interpreted the data with input from all other authors. C.J.H., S.N. R.S. and R.D.P. wrote the manuscript with contributions from all co-authors.

References

Aboglila, S., Grice, K., Trinajstic, K., Dawson, D., and Williford, K. H.: Use of biomarker distributions and compound specific isotopes of carbon and hydrogen to delineate hydrocarbon characteristics in the East Sirte Basin (Libya), Organic Geochemistry, 41, 1249-1258, https://doi.org/10.1016/j.orggeochem.2010.05.011, 2010.

Alexander, K., J. Meissner, K., and J. Bralower, T.: Sudden spreading of corrosive bottom water during the Palaeocene–Eocene Thermal Maximum, Nature Geoscience, 8, 458-461, 10.1038/ngeo2430, 2015.

Barnet, J. S. K., Littler, K., Westerhold, T., Kroon, D., Leng, M. J., Bailey, I., Röhl, U., and Zachos, J. C.: A high-fidelity benthic stable isotope record of Late Cretaceous–early Eocene climate change and carbon-cycling, Paleoceanography and Paleoclimatology, 34, 672-691, 10.1029/2019pa003556, 2019.

Batenburg, S. J., Voigt, S., Friedrich, O., Osborne, A. H., Bornemann, A., Klein, T., Pérez-Díaz, L., and Frank, M.: Major intensification of Atlantic overturning circulation at the onset of Paleogene greenhouse warmth, Nature Communications, 9, 4954, 10.1038/s41467-018-07457-7, 2018.

Beck, R. A., Burbank, D. W., Sercombe, W. J., Olson, T. L., and Khan, A. M.: Organic carbon exhumation and global warming during the early Himalayan collision, Geology, 23, 387-390, 10.1130/0091-7613(1995)023, 1995.

Bernaola, G., Baceta, J. I., Orue-Etxebarria, X., Alegret, L., MartÃ-n-Rubio, M., Arostegui, J., and DinarÃ¨s-Turell, J.: Evidence of an abrupt environmental disruption during the mid-Paleocene biotic event (Zumaia section, western Pyrenees), Geological Society of America Bulletin, 119, 785-795, 10.1130/b26132.1, 2007.

Bertoni, C., Gan, Y., Paganoni, M., Mayer, J., Cartwright, J., Martin, J., Van Rensbergen, P., Wunderlich, A., and Clare, A.: Late Paleocene pipe swarm in the Great South – Canterbury Basin (New Zealand), Marine and petroleum geology, 107, 451-466, https://doi.org/10.1016/j.marpetgeo.2019.05.039, 2019.

https://doi.org/10.5194/cp-2021-122
Preprint. Discussion started: 17 September 2021

Bidigare, R. R., Fluegge, A., Freeman, K. H., Hanson, K. L., Hayes, J. M., Hollander, D., Jasper, J. P., King, L. L., Laws, E. A., Milder, J., Millero, F. J., Pancost, R., Popp, B. N., Steinberg, P. A., and Wakeham, S. G.: Consistent fractionation of 13C in nature and in the laboratory: Growth-rate effects in some haptophyte algae, Global Biogeochemical Cycles, 11, 279-292, https://doi.org/10.1029/96GB03939, 1997.

Bijl, P. K., Frieling, J., Cramwinckel, M. J., Boschman, C., Sluijs, A., and Peterse, F.: Maastrichtian-Rupelian paleoclimates in the southwest Pacific – a critical evaluation of biomarker paleothermometry and dinoflagellate cyst paleoecology at Ocean Drilling Program Site 1172, Clim. Past Discuss., 2021, 1-82, 10.5194/cp-2021-18, 2021.

Bijl, P. K., Schouten, S., Sluijs, A., Reichart, G.-J., Zachos, J. C., and Brinkhuis, H.: Early Palaeogene temperature evolution of the southwest Pacific Ocean, Nature, 461, 776-779, 2009.

Brune, S., Williams, S. E., and Müller, R. D.: Potential links between continental rifting, CO2 degassing and climate change through time, Nature Geoscience, 10, 941-946, 10.1038/s41561-017-0003-6, 2017.

Carmichael, M. J., Inglis, G. N., Badger, M. P. S., Naafs, B. D. A., Behrooz, L., Remmelzwaal, S., Monteiro, F. M., Rohrssen, M., Farnsworth, A., Buss, H. L., Dickson, A. J., Valdes, P. J., Lunt, D. J., and Pancost, R. D.: Hydrological and associated biogeochemical consequences of rapid global warming during the Paleocene-Eocene Thermal Maximum, Global and Planetary Change, 157, 114-138, https://doi.org/10.1016/j.gloplacha.2017.07.014, 2017.

Clyde, W. C., Tong, Y., Snell, K. E., Bowen, G. J., Ting, S., Koch, P. L., Li, Q., Wang, Y., and Meng, J.: An integrated stratigraphic record from the Paleocene of the Chijiang Basin, Jiangxi Province (China): Implications for mammalian turnover and Asian block rotations, Earth and Planetary Science Letters, 269, 554-564, https://doi.org/10.1016/j.epsl.2008.03.009, 2008.

Contreras, L., Pross, J., Bijl, P. K., O'Hara, R. B., Raine, J. I., Sluijs, A., and Brinkhuis, H.: Southern high-latitude terrestrial climate change during the Palaeocene–Eocene derived from a marine pollen record (ODP Site 1172, East Tasman Plateau), Climate of the Past, 10, 1401-1420, 10.5194/cp-10-1401-2014, 2014.

Cook, R. A., Sutherland, R., and Zhu, H.: Cretaceous - Cenozoic geology and petroleum systems of the Great South Basin, New Zealand, Institute of Geological & Nuclear Sciences monograph, Institute of Geological & Nuclear Sciences, Lower Hutt, 190 p. 1999.

Corfield, R. M. and Cartlidge, J. E.: Oceanographic and climatic implications of the Palaeocene carbon isotope maximum, Terra Nova, 4, 443-455, 1992.

Corfield, R. M. and Norris, R. D.: Deep water circulation in the Paleocene ocean, in: Correlation of the early Paleogene in Northwest Europe, edited by: Knox, R. W. O. B., Corfield, R. M., and Dunay, R. E., Geological Society Special Publication No. 101, 443-456, 1996.

Crouch, E. M., Willumsen, P. S., Kulhanek, D. K., and Gibbs, S. J.: A revised Paleocene (Teurian) dinoflagellate cyst zonation from eastern New Zealand, Review of Palaeobotany and Palynology, 202, 47-79, https://doi.org/10.1016/j.revpalbo.2013.12.004, 2014.

Cui, Y. and Schubert, B. A.: Quantifying uncertainty of past pCO2 determined from changes in C3 plant carbon isotope fractionation, Geochimica et Cosmochimica Acta, 172, 127-138, https://doi.org/10.1016/j.gca.2015.09.032, 2016.

Cui, Y. and Schubert, B. A.: Atmospheric pCO2 reconstructed across five early Eocene global warming events, Earth and Planetary Science Letters, 478, 225-233, https://doi.org/10.1016/j.epsl.2017.08.038, 2017.

Cui, Y. and Schubert, B. A.: Towards determination of the source and magnitude of atmospheric pCO2 change across the early Paleogene hyperthermals, Global and Planetary Change, 170, 120-125, https://doi.org/10.1016/j.gloplacha.2018.08.011, 2018.

https://doi.org/10.5194/cp-2021-122
Preprint. Discussion started: 17 September 2021

Dawson, D., Grice, K., and Alexander, R.: Effect of maturation on the indigenous δD signatures of individual hydrocarbons in sediments and crude oils from the Perth Basin (Western Australia), Organic Geochemistry, 36, 95-104, https://doi.org/10.1016/j.orggeochem.2004.06.020, 2005.

De Conto, R. M., Galeotti, S., Pagani, M., Tracy, D., Schaefer, K., Zhang, T., Pollard, D., and Beerling, D. J.: Past extreme warming events linked to massive carbon release from thawing permafrost, Nature, 484, 87-91, http://www.nature.com/nature/journal/v484/n7392/abs/nature10929.html#supplementary-information, 2012.

Dickens, G. R.: Rethinking the global carbon cycle with a large, dynamic and microbially mediated gas hydrate capacitor, Earth and Planetary Science Letters, 213, 169-183, 2003.

Fernandez, I., Mahieu, N., and Cadisch, G.: Carbon isotopic fractionation during decomposition of plant materials of different quality, Global Biogeochemical Cycles, 17, https://doi.org/10.1029/2001GB001834, 2003.

Field, B. D., Browne, G., et al..: Cretaceous Cenozoic sedimentary basins and geological evolution of the Canterbury region, South Island, New Zealand, New Zealand Geological Survey basin studies, vol. 2, New Zealand Geological Survey, Lower Hutt, 94 pp., 1989.

Field, B. D., Uruski, C. I., et al.: Cretaceous-Cenozoic geology and petroleum systems of the East Coast Region, Institute of Geological and Nuclear Sciences monograph 19, Institute of Geological and Nuclear Sciences Limited, Lower Hutt, 301 pp., 1997.

Field, B. D., Naeher, S., Clowes, C. D., Shepherd, C. L., Hollis, C. J., Sykes, R., Ventura, G. T., Pascher, K. M., and Griffin, A. C.: Depositional Influences on the Petroleum Potential of the Waipawa Formation in the Orui-1A Drillhole, Wairarapa, GNS Science Report 2017/49, 75 pp., 2018.

Foster, G. L., Royer, D. L., and Lunt, D. J.: Future climate forcing potentially without precedent in the last 420 million years, Nature Communications, 8, 14845, 10.1038/ncomms14845, 2017.

Freeman, K. H. and Hayes, J. M.: Fractionation of carbon isotopes by phytoplankton and estimates of ancient CO_2 levels, Global Biogeochemical Cycles, 6, 185-198, 1992.

Gradstein, F. M., Ogg, J. G., Schmitz, M., and Ogg, G.: The Geologic Time Scale 2012, Elsevier, Amsterdam, 1176 pp., 2012.

Grice, K., Mesmay, R. d., Glucina, A., and Wang, S.: An improved and rapid 5A molecular sieve method for gas chromatography isotope ratio mass spectrometry of *n*-alkanes (C_8–C^{30+}), Organic Geochemistry, 39, 284-288, https://doi.org/10.1016/j.orggeochem.2007.12.009, 2008.

Gröcke, D. R.: Carbon isotope analyses of fossil plants as a chemostratigraphic and palaeoenvironmental tool, Lethaia, 31, 1-13, 1998.

Gröcke, D. R., Hesselbo, S. P., and Jenkyns, H. C.: Carbon-isotope composition of Lower Cretaceous fossil wood: Ocean-atmosphere chemistry and relation to sea-level change, Geology, 27, 155-158, 1999.

Hardenbol, J., Thierry, J., Farley, M. B., de Graciansky, P.-C., and Vail, P. R.: Mesozoic and Cenozoic sequence chronostratigraphic framework of European basins, in: Mesozoic and Cenozoic sequence stratigraphy of European basins. SEPM Special Publication 60, edited by: de Graciansky, P.-C., Hardenbol, J., Jacquin, T., and Vail, P. R., 3-13, 1998.

Harris, A. D., Miller, K. G., Browning, J. V., Sugarman, P. J., Olsson, R. K., Cramer, B. S., and Wright, J. D.: Integrated stratigraphic studies of Paleocene-lowermost Eocene sequences, New Jersey Coastal Plain: Evidence for glacioeustatic control, Paleoceanography, 25, PA3211, 10.1029/2009pa001800, 2010.

Hayes, J. M.: Factors controlling ^{13}C contents of sedimentary organic compounds: Principles and evidence, Marine Geology, 113, 111-125, 1993.

Hayward, B. W.: A guide to paleoenvironmental assessment using New Zealand Cenozoic foraminiferal faunas, New Zealand Geological Survey PAL report, 109, 1-73, 1986.

https://doi.org/10.5194/cp-2021-122
Preprint. Discussion started: 17 September 2021

Hedges, J. I., Cowie, G. L., Ertel, J. R., James Barbour, R., and Hatcher, P. G.: Degradation of carbohydrates and lignins in buried woods, Geochimica et Cosmochimica Acta, 49, 701-711, https://doi.org/10.1016/0016-7037(85)90165-6, 1985.

Hill, P. J. and Exon, N. F.: Tectonics and Basin Development of the Offshore Tasmanian Area Incorporating Results from Deep Ocean Drilling, in: The Cenozoic Southern Ocean: Tectonics, Sedimentation, and Climate Change Between Australia and Antarctica, 19-42, https://doi.org/10.1029/151GM03, 2004.

Hilting, A. K., Kump, L. R., and Bralower, T. J.: Variations in the oceanic vertical carbon isotope gradient and their implications for the Paleocene-Eocene biological pump, Paleoceanography, 23, 10.1029/2007pa001458, 2008.

Hines, B. R., Gazley, M. F., Collins, K. S., Bland, K. J., Crampton, J. S., and Ventura, G. T.: Chemostratigraphic resolution of widespread reducing conditions in the southwest Pacific Ocean during the Late Paleocene, Chemical Geology, 504, 236-252, https://doi.org/10.1016/j.chemgeo.2018.11.020, 2019.

Hollis, C. J., Field, B. D., Crouch, E. M., and Sykes, R.: How good a source rock is the Waipawa (black shale) Formation beyond the East Coast Basin? An outcrop-based case study from Northland, in: New Zealand Petroleum Conference 2006 (Auckland, NZ), 8 p., 2006.

Hollis, C. J., Dickens, G. R., Field, B. D., Jones, C. J., and Strong, C. P.: The Paleocene-Eocene transition at Mead Stream, New Zealand: a southern Pacific record of early Cenozoic global change, Palaeogeography, Palaeoclimatology, Palaeoecology, 215, 313-343, 2005.

Hollis, C. J., Taylor, K. W. T., Handley, L., Pancost, R. D., Huber, M., Creech, J., Hines, B., Crouch, E. M., Morgans, H. E. G., Crampton, J. S., Gibbs, S., Pearson, P., and Zachos, J. C.: Early Paleogene temperature history of the Southwest Pacific Ocean: reconciling proxies and models, Earth and Planetary Science Letters, 349-350, 53-66, 2012.

Hollis, C. J., Tayler, M. J. S., Andrew, B., Taylor, K. W., Lurcock, P., Bijl, P. K., Kulhanek, D. K., Crouch, E. M., Nelson, C. S., Pancost, R. D., Huber, M., Wilson, G. S., Ventura, G. T., Crampton, J. S., Schiøler, P., and Phillips, A.: Organic-rich sedimentation in the South Pacific Ocean associated with Late Paleocene climatic cooling, Earth-Science Reviews, 134, 81-97, http://dx.doi.org/10.1016/j.earscirev.2014.03.006, 2014.

Hollis, C. J., Dunkley Jones, T., Anagnostou, E., Bijl, P. K., Cramwinckel, M. J., Cui, Y., Dickens, G. R., Edgar, K. M., Eley, Y., Evans, D., Foster, G. L., Frieling, J., Inglis, G. N., Kennedy, E. M., Kozdon, R., Lauretano, V., Lear, C. H., Littler, K., Lourens, L., Meckler, A. N., Naafs, B. D. A., Pälike, H., Pancost, R. D., Pearson, P. N., Röhl, U., Royer, D. L., Salzmann, U., Schubert, B. A., Seebeck, H., Sluijs, A., Speijer, R. P., Stassen, P., Tierney, J., Tripati, A., Wade, B., Westerhold, T., Witkowski, C., Zachos, J. C., Zhang, Y. G., Huber, M., and Lunt, D. J.: The DeepMIP contribution to PMIP4: methodologies for selection, compilation and analysis of latest Paleocene and early Eocene climate proxy data, incorporating version 0.1 of the DeepMIP database, Geosci. Model Dev., 12, 3149-3206, 10.5194/gmd-12-3149-2019, 2019.

Holman, A. I. and Grice, K.: δ13C of aromatic compounds in sediments, oils and atmospheric emissions: A review, Organic Geochemistry, 123, 27-37, https://doi.org/10.1016/j.orggeochem.2018.06.004, 2018.

Hyland, E. G., Sheldon, N. D., and Cotton, J. M.: Terrestrial evidence for a two-stage mid-Paleocene biotic event, Palaeogeography, Palaeoclimatology, Palaeoecology, 417, 371-378, https://doi.org/10.1016/j.palaeo.2014.09.031, 2015.

Isaac, M. J., Herzer, R. H., Brook, F. J., and Hayward, B. W.: Cretaceous and Cenozoic sedimentary basins of Northland, New Zealand, Institute of Geological & Nuclear Sciences Monograph, vol. 8, 230 pp.1994.

Killops, S. D., Hollis, C. J., Morgans, H. E. G., Sutherland, R., Field, B. D., and Leckie, D. A.: Paleoceanographic significance of Late Paleocene dysaerobia at the shelf/slope break around New Zealand, Palaeogeography, Palaeoclimatology, Palaeoecology, 156, 51-70, 2000.

https://doi.org/10.5194/cp-2021-122
Preprint. Discussion started: 17 September 2021

King, P. R., Naish, T. R., Browne, G. H., Field, B. D., and Edbrooke, S. W.: Cretaceous to Recent sedimentary patterns in New Zealand, Institute of Geological and Nuclear Sciences folio series 1, Institute of Geological and Nuclear Sciences folio series 1, 35 pp., 1999.

Kominz, M. A., Browning, J. V., Miller, K. G., Sugarman, P. J., Mizintseva, S., and Scotese, C. R.: Late Cretaceous to Miocene sea-level estimates from the New Jersey and Delaware coastal plain coreholes: an error analysis, Basin Research, 20, 211-226, 10.1111/j.1365-2117.2008.00354.x, 2008.

Kulhanek, D. K., Crouch, E. M., Tayler, M. J. S., and Hollis, C. J.: Paleocene calcareous nannofossils from East Coast, New Zealand: Biostratigraphy and paleoecology, Journal of Nannoplankton Research, 35, 155-176, 2015.

Kurtz, A. C., Kump, L. R., Arthur, M. A., Zachos, J. C., and Paytan, A.: Early Cenozoic decoupling of the global carbon and sulfur cycles, Paleoceanography, 18, 1090, doi:1010.1029/2003PA000908, 2003.

Littler, K., Röhl, U., Westerhold, T., and Zachos, J. C.: A high-resolution benthic stable-isotope record for the South Atlantic: Implications for orbital-scale changes in Late Paleocene–Early Eocene climate and carbon cycling, Earth and Planetary Science Letters, 401, 18-30, https://doi.org/10.1016/j.epsl.2014.05.054, 2014.

Lomax, B. H., Lake, J. A., Leng, M. J., and Jardine, P. E.: An experimental evaluation of the use of Δ13C as a proxy for palaeoatmospheric CO2, Geochimica et Cosmochimica Acta, 247, 162-174, https://doi.org/10.1016/j.gca.2018.12.026, 2019.

Moore, P. R.: Stratigraphy, composition, and environment of deposition of the Whangai Formation and associated Late Cretaceous-Paleocene rocks, eastern North Island, New Zealand. New Zealand Geological Survey Bulletin 100, 82 pp., 1988.

Naeher, S., Hollis, C. J., Clowes, C. D., Ventura, G. T., Shepherd, C. L., Crouch, E. M., Morgans, H. E. G., Bland, K. J., Strogen, D. P., and Sykes, R.: Depositional and organofacies influences on the petroleum potential of an unusual marine source rock: Waipawa Formation (Paleocene) in southern East Coast Basin, New Zealand, Marine and petroleum geology, https://doi.org/10.1016/j.marpetgeo.2019.03.035, 2019.

Pancost, R. D., Freeman, K. H., and Patzkowsky, M. E.: Organic-matter source variation and the expression of a late Middle Ordovician carbon isotope excursion, Geology, 27, 1015-1018, 1999.

Pancost, R. D., Taylor, K. W. R., and Hollis, C. J.: A critical evaluation of TEX_{86} derived sea surface temperatures in the Paleogene, Goldschmidt Conference, 2012.

Pancost, R. D., Telnæs, N., and Sinninghe Damsté, J. S.: Carbon isotopic composition of an isoprenoid-rich oil and its potential source rock, Organic Geochemistry, 32, 87-103, https://doi.org/10.1016/S0146-6380(00)00149-2, 2001.

Peters, K. E., Walters, C. C., and Moldowan, J. M.: The biomarker guide: 1. Biomarkers and isotopes in the environment and human history, Cambridge University Press, Cambridge, UK2005.

Petrizzo, M.: An early late Paleocene event on Shatsky Rise, northwest Pacific Ocean (ODP Leg 198): evidence from planktonic foraminiferal assemblages, in: Proc. ODP, Sci. Results, edited by: Bralower, T. J., Premoli Silva, I., and Malone, M., Ocean Drilling Program, College Station, 1–29. doi:10.2973/odp.proc.sr.2198.2102.2005, 2005.

Rosenberg, Y. O., Kutuzov, I., and Amrani, A.: Sulfurization as a preservation mechanism for the δ13C of biomarkers, Organic Geochemistry, 125, 66-69, https://doi.org/10.1016/j.orggeochem.2018.08.010, 2018.

Rotich, E. K., Handler, M. R., Naeher, S., Selby, D., Hollis, C. J., and Sykes, R.: Re-Os geochronology and isotope systematics, and organic and sulfur geochemistry of the middle–late Paleocene Waipawa Formation, New Zealand: Insights into early Paleogene seawater Os isotope composition, Chemical Geology, 536, 119473, https://doi.org/10.1016/j.chemgeo.2020.119473, 2020.

Saller, A., Lin, R., and Dunham, J.: Leaves in turbidite sands: The main source of oil and gas in the deep-water Kutei Basin, Indonesia, AAPG Bulletin, 90, 1585-1608, 10.1306/04110605127, 2006.

https://doi.org/10.5194/cp-2021-122
Preprint. Discussion started: 17 September 2021

Schiøler, P.: Palynofacies and sequence stratigraphy of the Late Cretaceous to Paleogene succession in the Galleon-1 and Resolution-1 wells, Canterbury Basin, New Zealand, GNS Science Consultancy Report (open file) 2011/123, GNS Science, Lower Hutt, 38 pp., 2011.

Schiøler, P., Rogers, K., Sykes, R., Hollis, C. J., Ilg, B., Meadows, D., Roncaglia, L., and Uruski, C.: Palynofacies, organic geochemistry and depositional environment of the Tartan Formation (Late Paleocene), a potential source rock in the Great South Basin, New Zealand, Marine and Petroleum Geology, 27, 351-369, doi:10.1016/j.marpetgeo.2009.09.006, 2010.

Schlanser, K., Diefendorf, A. F., Greenwood, D. R., Mueller, K. E., West, C. K., Lowe, A. J., Basinger, J. F., Currano, E. D., Flynn, A. G., Fricke, H. C., Geng, J., Meyer, H. W., and Peppe, D. J.: On geologic timescales, plant carbon isotope fractionation responds to precipitation similarly to modern plants and has a small negative correlation with pCO2, Geochimica et Cosmochimica Acta, 270, 264-281, https://doi.org/10.1016/j.gca.2019.11.023, 2020.

Schleser, G. H., Frielingsdorf, J., and Blair, A.: Carbon isotope behaviour in wood and cellulose during artificial aging, Chemical Geology, 158, 121-130, https://doi.org/10.1016/S0009-2541(99)00024-8, 1999.

Schouten, S., Woltering, M., Rijpstra, W. I. C., Sluijs, A., Brinkhuis, H., and Sinninghe Damsté, J. S.: The Paleocene–Eocene carbon isotope excursion in higher plant organic matter: Differential fractionation of angiosperms and conifers in the Arctic, Earth and Planetary Science Letters, 258, 581-592, https://doi.org/10.1016/j.epsl.2007.04.024, 2007.

Schubert, B. A. and Jahren, A. H.: The effect of atmospheric CO2 concentration on carbon isotope fractionation in C3 land plants, Geochimica et Cosmochimica Acta, 96, 29-43, https://doi.org/10.1016/j.gca.2012.08.003, 2012.

Schubert, B. A. and Jahren, A. H.: Incorporating the effects of photorespiration into terrestrial paleoclimate reconstruction, Earth-Science Reviews, 177, 637-642, https://doi.org/10.1016/j.earscirev.2017.12.008, 2018.

Schweizer, M., Fear, J., Cadisch, G.: Isotopic (^{13}C) fractionation during plant residue decomposition and its implications for soil organic matter studies, Rapid Communications in Mass Spectrometry, 13, 1284-1290, 1999.

Sexton, P. F., Norris, R. D., Wilson, P. A., Palike, H., Westerhold, T., Rohl, U., Bolton, C. T., and Gibbs, S.: Eocene global warming events driven by ventilation of oceanic dissolved organic carbon, Nature, 471, 349-352, 2011.

Sinninghe Damsté , J. S., Kok, M. D., Köster, J., and Schouten, S.: Sulfurized carbohydrates: an important sedimentary sink for organic carbon?, Earth and Planetary Science Letters, 164, 7-13, 1998.

Sinninghe Damsté, J. S., van Bentum, E. C., Reichart, G.-J., Pross, J., and Schouten, S.: A CO_2 decrease-driven cooling and increased latitudinal temperature gradient during the mid-Cretaceous Oceanic Anoxic Event 2, Earth and Planetary Science Letters, 293, 97-103, https://doi.org/10.1016/j.epsl.2010.02.027, 2010.

Sluijs, A. and Dickens, G. R.: Assessing offsets between the $\delta^{13}C$ of sedimentary components and the global exogenic carbon pool across early Paleogene carbon cycle perturbations, Global Biogeochemical Cycles, 26, GB4005, doi: 4010.1029/2011gb004224, 10.1029/2011gb004224, 2012.

Sofer, Z.: Stable Carbon Isotope Compositions of Crude Oils: Application to Source Depositional Environments and Petroleum Alteration1, AAPG Bulletin, 68, 31-49, 10.1306/ad460963-16f7-11d7-8645000102c1865d, 1984.

Speijer, R. P., Pälike, H., Hollis, C. J., Hooker, J. J., and Ogg, J. G.: Chapter 28 - The Paleogene Period, in: Geologic Time Scale 2020, edited by: Gradstein, F. M., Ogg, J. G., Schmitz, M. D., and Ogg, G. M., Elsevier, 1087-1140, https://doi.org/10.1016/B978-0-12-824360-2.00028-0, 2020.

Sykes, R., Zink, K.-G.: The New Zealand Source Rock Extracts Database. GNS Science Data Series 14c, New Zealand Petroleum Report, 4516, 2012.

Sykes, R. R., K.M.; Phillips, A.; Zink, K.-G.; Ventura, G.T.: The New Zealand Petroleum Carbon and Hydrogen Isotope Database. GNS Science Data Series 14d, New Zealand Petroleum Report, 4517, 2012.

https://doi.org/10.5194/cp-2021-122
Preprint. Discussion started: 17 September 2021

Tayler, M. J. S.: Investigating stratigraphic evidence for Antarctic glaciation in the greenhouse world of the Paleocene, eastern North Island, New Zealand, Earth and Ocean Sciences, University of Waikato, Hamilton, 292 pp., 2011.

Taylor, K.: Paleocene climate and carbon cycle: insights into an unstable greenhouse from a biomarker and compound specific carbon isotope approach, University of Bristol, Bristol, 310 pp., 2011.

Taylor, K. W. R., Willumsen, P. S., Hollis, C. J., and Pancost, R. D.: South Pacific evidence for the long-term climate impact of the Cretaceous/Paleogene boundary event, Earth-Science Reviews, 179, 287-302, https://doi.org/10.1016/j.earscirev.2018.02.012, 2018.

Thomas, D. J., Korty, R., Huber, M., Schubert, J. A., and Haines, B.: Nd isotopic structure of the Pacific Ocean 70–30 Ma and numerical evidence for vigorous ocean circulation and ocean heat transport in a greenhouse world, Paleoceanography, 29, 454-469, 10.1002/2013pa002535, 2014.

Urban, M. A., Nelson, D. M., Jiménez-Moreno, G., Châteauneuf, J.-J., Pearson, A., and Hu, F. S.: Isotopic evidence of C4 grasses in southwestern Europe during the Early Oligocene–Middle Miocene, Geology, 38, 1091-1094, 10.1130/g31117.1, 2010.

van Bergen, P. F. and Poole, I.: Stable carbon isotopes of wood: a clue to palaeoclimate?, Palaeogeography, palaeoclimatology, palaeoecology, 182, 31-45, https://doi.org/10.1016/S0031-0182(01)00451-5, 2002.

Van Kaam-Peters, H. M. E., Schouten, S., Köster, J., and Sinninghe Damstè, J. S.: Controls on the molecular and carbon isotopic composition of organic matter deposited in a Kimmeridgian euxinic shelf sea: evidence for preservation of carbohydrates through sulfurisation, Geochimica et Cosmochimica Acta, 62, 3259-3283, https://doi.org/10.1016/S0016-7037(98)00231-2, 1998.

Westerhold, T., Röhl, U., Donner, B., and Zachos, J. C.: Global extent of early Eocene hyperthermal events: A new Pacific benthic foraminiferal isotope record from Shatsky Rise (ODP Site 1209), Paleoceanography and Paleoclimatology, 33, 626-642, doi:10.1029/2017PA003306, 2018.

Westerhold, T., Röhl, U., Donner, B., McCarren, H. K., and Zachos, J. C.: A complete high-resolution Paleocene benthic stable isotope record for the central Pacific (ODP Site 1209), Paleoceanography, 26, PA2216, 10.1029/2010pa002092, 2011.

Westerhold, T., Röhl, U., Frederichs, T., Agnini, C., Raffi, I., Zachos, J. C., and Wilkens, R. H.: Astronomical calibration of the Ypresian timescale: implications for seafloor spreading rates and the chaotic behavior of the solar system?, Climate of the Past, 13, 1129-1152, 10.5194/cp-13-1129-2017, 2017.

Westerhold, T., Röhl, U., Raffi, I., Fornaciari, E., Monechi, S., Reale, V., Bowles, J., and Evans, H. F.: Astronomical calibration of the Paleocene time, Palaeogeography, palaeoclimatology, palaeoecology, 257, 377-403, 2008.

Westerhold, T., Marwan, N., Drury, A. J., Liebrand, D., Agnini, C., Anagnostou, E., Barnet, J. S. K., Bohaty, S. M., De Vleeschouwer, D., Florindo, F., Frederichs, T., Hodell, D. A., Holbourn, A. E., Kroon, D., Lauretano, V., Littler, K., Lourens, L. J., Lyle, M., Pälike, H., Röhl, U., Tian, J., Wilkens, R. H., Wilson, P. A., and Zachos, J. C.: An astronomically dated record of Earth's climate and its predictability over the last 66 million years, Science, 369, 1383-1387, 10.1126/science.aba6853, 2020.

Zachos, J. C., Dickens, G. R., and Zeebe, R. E.: An early Cenozoic perspective on greenhouse warming and carbon-cycle dynamics, Nature, 451, 279-283, 2008.

Zachos, J. C., Röhl, U., Schellenberg, S. A., Sluijs, A., Hodell, D. A., Kelly, D. C., Thomas, E., Nicolo, M., Raffi, I., Lourens, L. J., McCarren, H., and Kroon, D.: Rapid Acidification of the Ocean During the Paleocene-Eocene Thermal Maximum, Science, 308, 1611-1615, 10.1126/science.1109004, 2005.

https://doi.org/10.5194/cp-2021-122
Preprint. Discussion started: 17 September 2021

Climate of the Past Discussions
Open Access
EGU

895 **Figures**

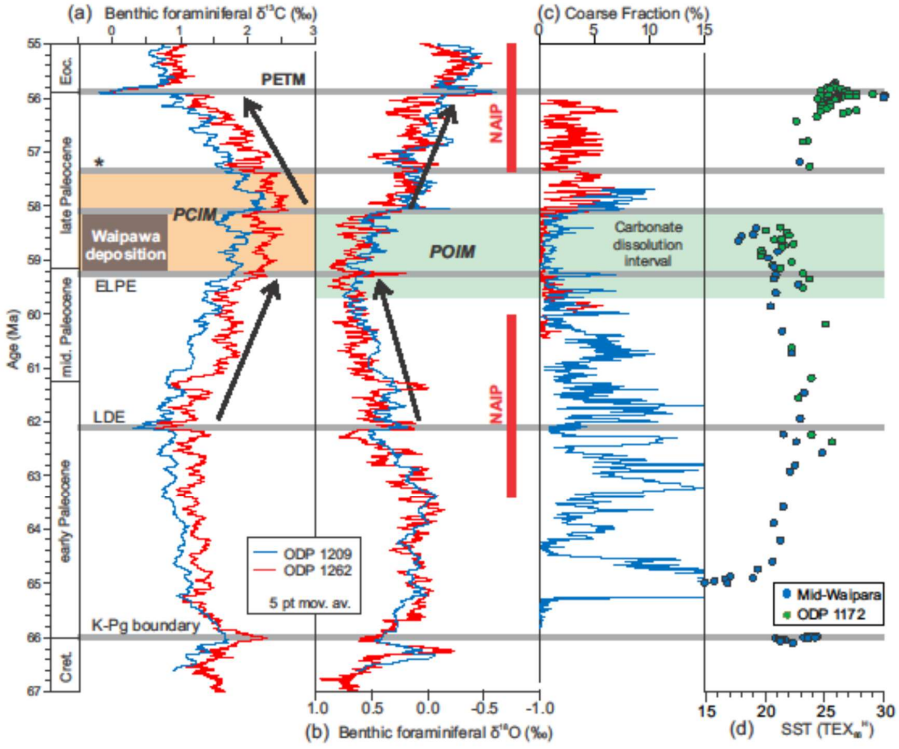

Figure 1. Paleocene variation in benthic foraminiferal carbon (a) and oxygen (b) stable isotopes and sediment coarse fraction (>63 µm) percentage (c) for ODP sites 1209 and 1262 (from Barnet et al., 2019) compared with variation in TEX_{86}^{H}-derived SST estimates from ODP Site 1172 and mid-Waipara River (from Hollis et al., 2012, 2014, 2019). Climatic and biotic events highlighted
900 **are the Cretaceous/Paleogene (K/Pg) boundary, Late Danian Event (LDE), early late Paleocene event (ELPE), Paleocene oxygen isotope maximum (POIM), Paleocene carbon isotope maximum (PCIM) and Paleocene-Eocene thermal maximum (PETM); North Atlantic Igneous Province (NAIP) eruptive phases. Timing of Waipawa organofacies deposition is also shown.**

https://doi.org/10.5194/cp-2021-122
Preprint. Discussion started: 17 September 2021

Climate of the Past Discussions
Open Access
EGU

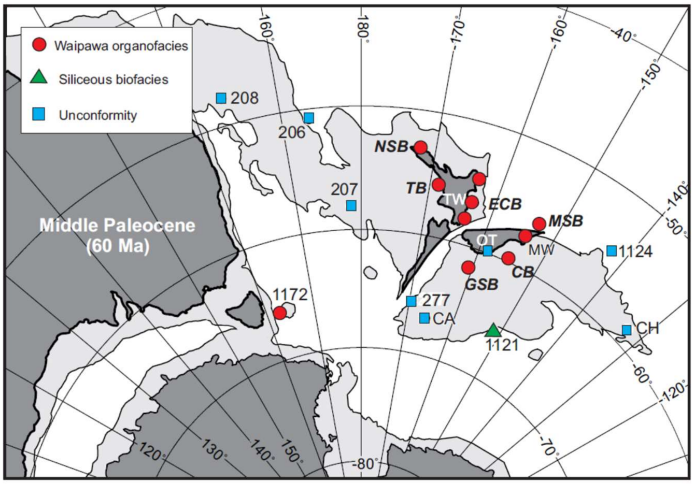

905

Figure 2. Localities where Waipawa organofacies is present or represented by an unconformity or a correlated siliceous biofacies on a middle Paleocene paleogeographic reconstruction (from Hollis et al., 2014). Locality abbreviations: NSB, North Slope Basin; TB, Taranaki Basin; TW, Taylor White section; ECB, East Coast Basin; MSB, Marlborough Sub-basin; MW, mid-Waipara section; CB, Canterbury basin; OT, onshore Otago; GSB, Great South Basin; CH, Chatham Island; CA, Campbell Island.

910 **Numbers refer to DSDP/ODP sites. See Fig. S1 for present-day section locations.**

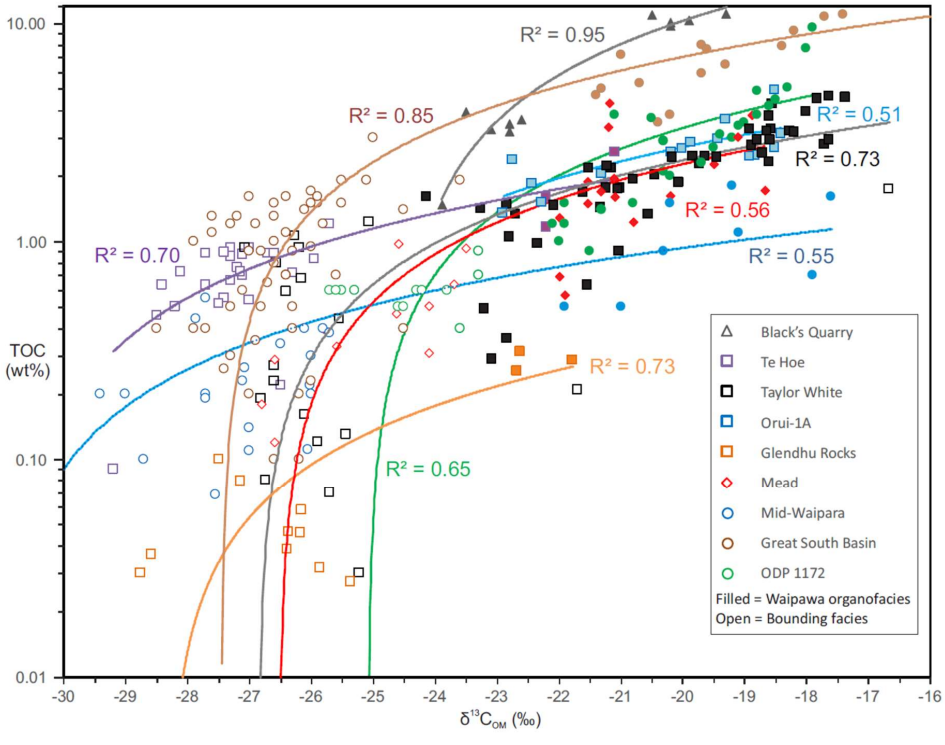

Figure 3. Correlation between TOC and $\delta^{13}C_{OM}$ in the studied sections. Correlation coefficients (R^2) relate to the linear regression lines of the same colour. Great South Basin (GSB) drillholes include Hoiho-1C, Kawau-1A, Pakaha-1 and Toroa-1.

https://doi.org/10.5194/cp-2021-122
Preprint. Discussion started: 17 September 2021

Climate of the Past Discussions
Open Access
EGU

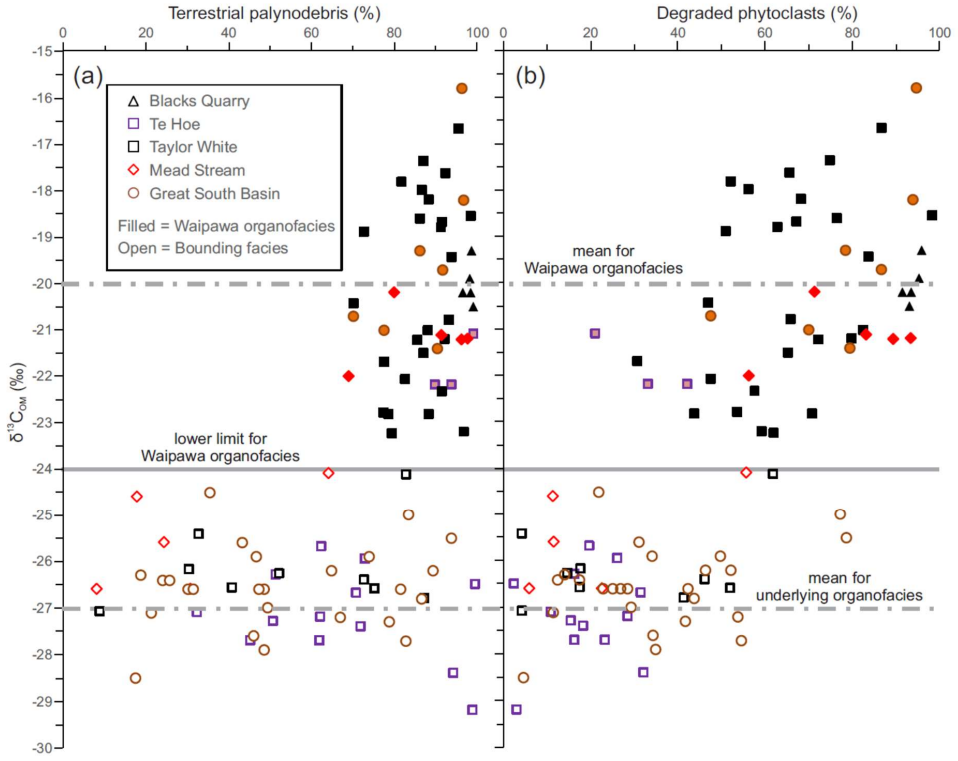

915 **Figure 4. Correlation of $\delta^{13}C_{OM}$ with (a) terrestrial palynodebris and (b) degraded phytoclasts in five onshore sections and four drillholes in the Great South Basin (Toroa-1, Pakaha-1, Kawau-1A and Hoiho-1C).**

https://doi.org/10.5194/cp-2021-122
Preprint. Discussion started: 17 September 2021

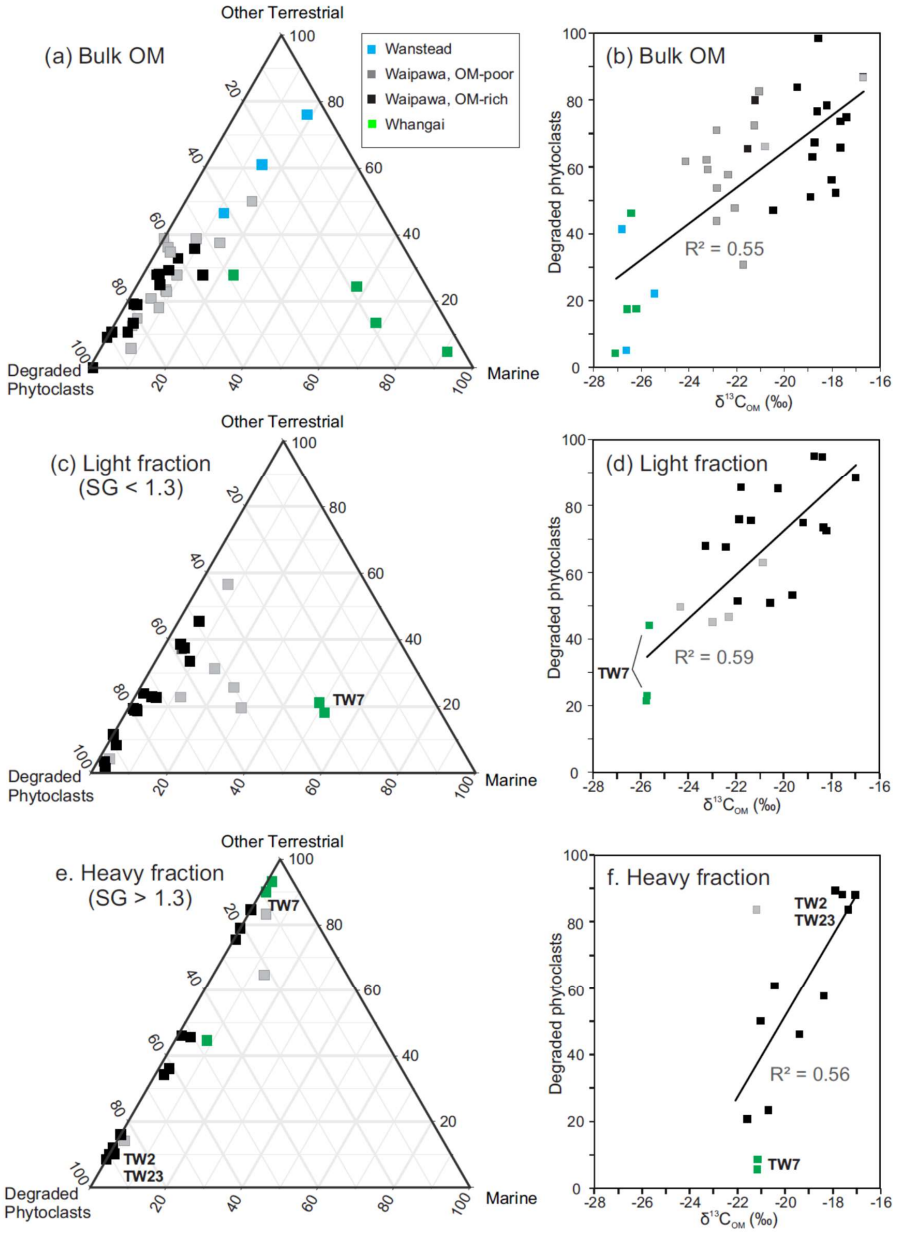

Figure 5. Proportions of primary palynofacies components (degraded phytoclasts, other terrestrial, marine) in (a) bulk organic matter and (c) light and (e) heavy density fractions compared with cross-plots of degraded phytoclasts and $\delta^{13}C_{OM}$ for (b) bulk organic matter and (d) light and (f) heavy density fractions for samples from four facies in the Taylor White section. Selected samples referred to in text are annotated. Density fractions were unavailable for Wanstead and some Whangai samples because of low OM contents.

https://doi.org/10.5194/cp-2021-122
Preprint. Discussion started: 17 September 2021

Climate of the Past Discussions

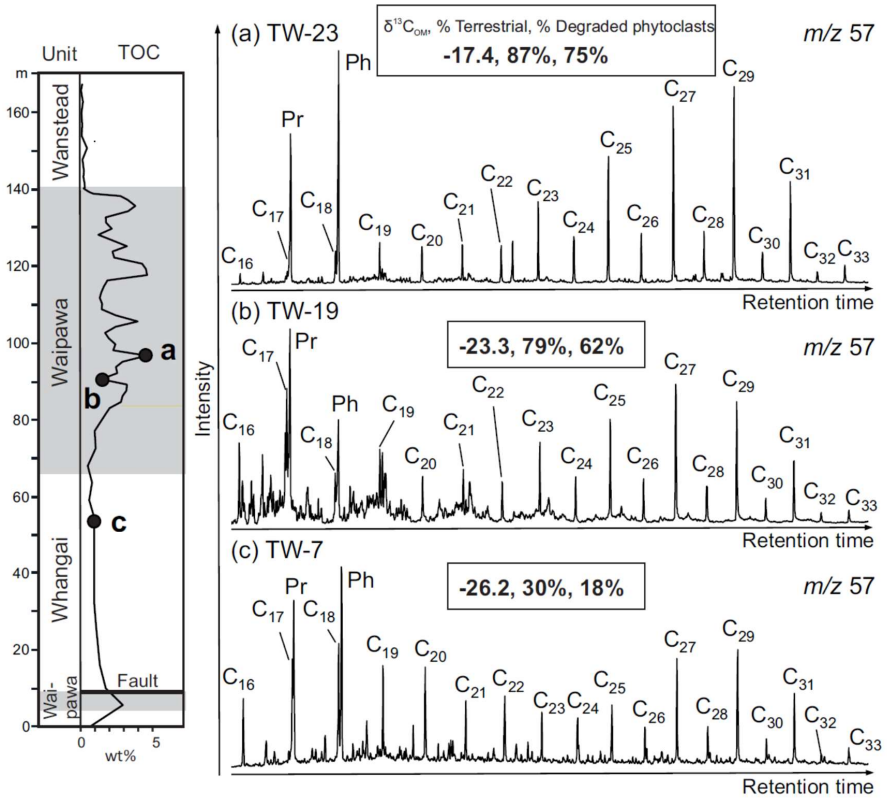

Figure 6. Representative biomarker chromatograms for (a) organic-rich Waipawa facies, (b) organic-poor Waipawa facies and (c) Whangai facies in the Taylor White section. The $\delta^{13}C_{OM}$ value and percentages of terrestrial palynodebris and degraded phytoclasts are also shown for each sample. Identified peaks are *n*-alkanes, pristane (Pr) and phytane (Ph).

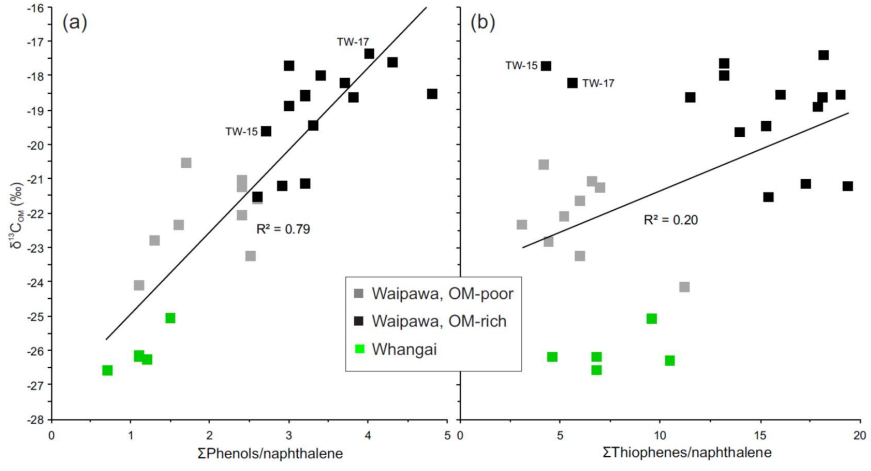

Figure 7. Correlation of $\delta^{13}C_{OM}$ with (a) phenol and (b) thiophene abundances relative to naphthalene for the OM-rich (TOC >2 wt%) and OM-poor (TOC <2 wt%) Waipawa facies and Whangai facies in the Taylor White section. The indicated linear regressions include all samples. The two outlier OM-rich Waipawa samples TW-15 and -17 are from just above the transition zone beneath the main Waipawa interval and therefore may not be fully representative of the end-member-type Waipawa organofacies.

https://doi.org/10.5194/cp-2021-122
Preprint. Discussion started: 17 September 2021

Climate of the Past Discussions
Open Access
EGU

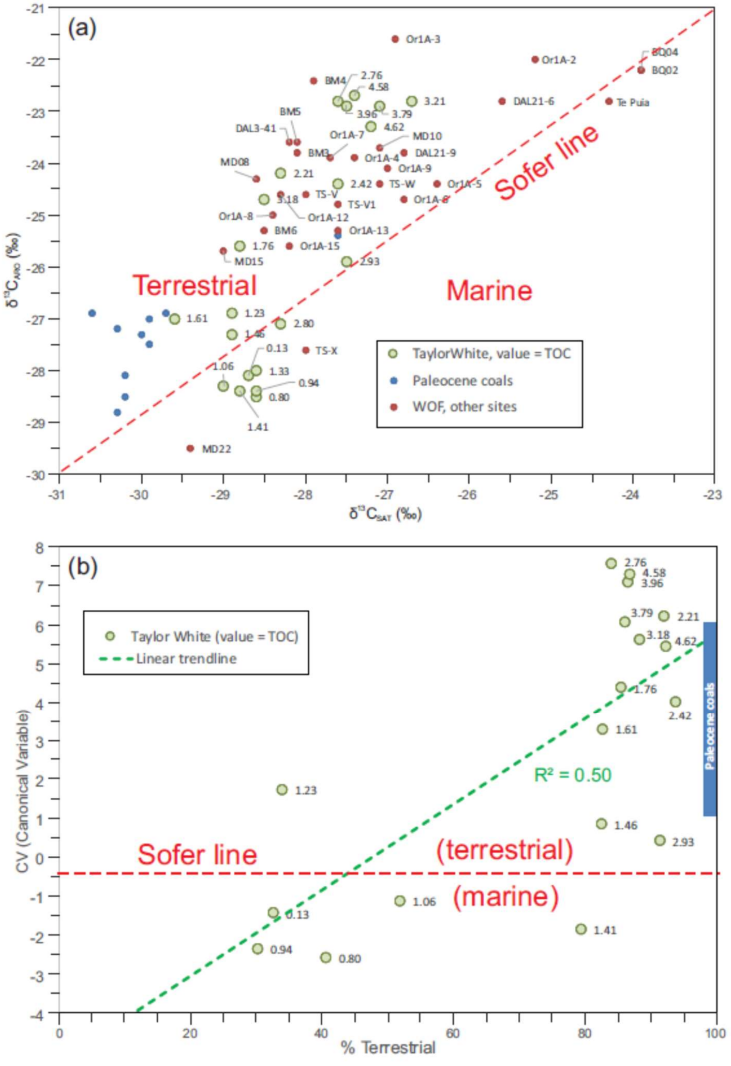

Figure 8. Relationship between $\delta^{13}C$ values for aromatic and saturated hydrocarbon fractions for the OM-rich (TOC >2 wt%) and OM-poor (TOC <2 wt%) Waipawa facies and Whangai facies in the Taylor White section shown as (a) a cross-plot of the two variables (selected samples referred to in the text are annotated with sample numbers and TOC values) and (b) a cross-plot of the percentage of terrestrial palynodebris and the canonical variable (samples labelled with TOC values). Samples of OM-rich Waipawa facies from other sections (in (a) only) and Paleocene coaly rocks are included for comparison (see Table S4 for sample details). The Sofer line and canonical variable provide distinction of marine and terrestrial OM sources (Sofer, 1984).

https://doi.org/10.5194/cp-2021-122
Preprint. Discussion started: 17 September 2021

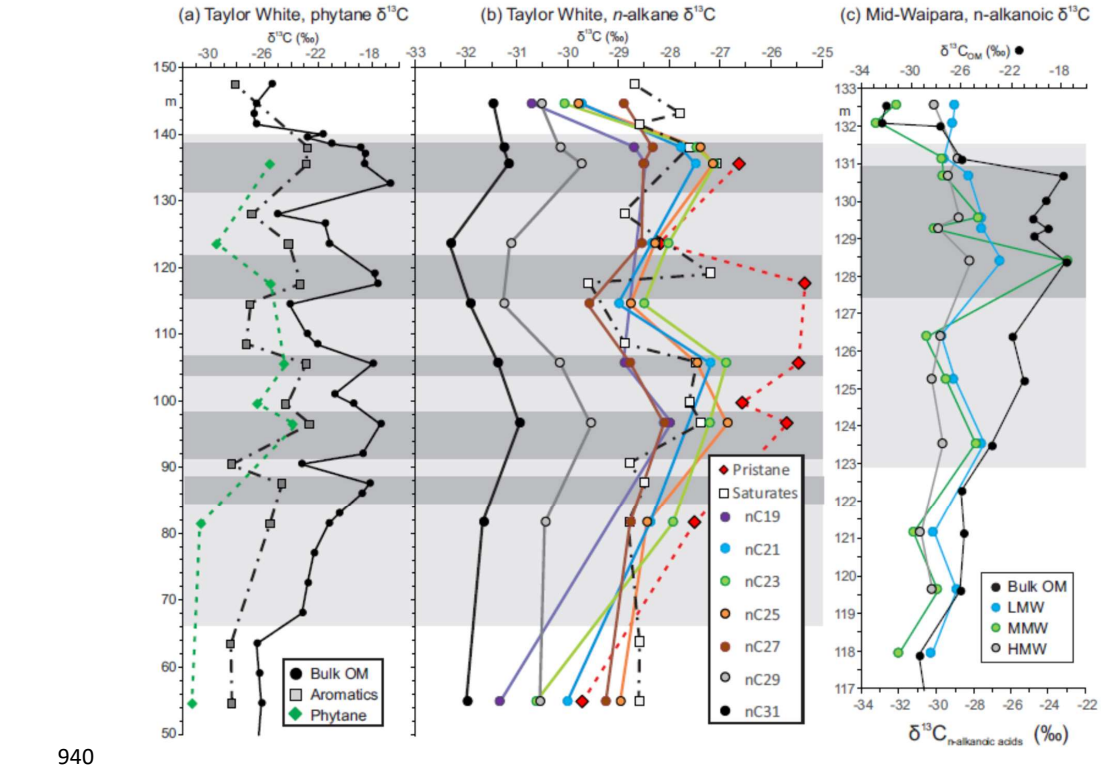

940 **Figure 9.**

Stratigraphic and facies-related variation in compound-specific $\delta^{13}C$ values in the (a, b) Taylor White and (c) mid-Waipara sections compared with $\delta^{13}C_{OM}$ in the two sections (a, c) and $\delta^{13}C$ of aromatic and saturated hydrocarbons in the Taylor White section (a, b): (a) phytane; (b) pristane and six representative *n*-alkanes (nC_{19}, nC_{21}, nC_{23}, nC_{25}, nC_{27}, nC_{29}, nC_{31}); (c) mean values for low molecular weight (LMW: nC_{16}, nC_{18}), medium molecular weight (MMW: nC_{20}, nC_{22}, nC_{24}, nC_{26}) and high molecular

945 **weight (HMW: nC_{30}, nC_{32}) fatty or *n*-alkanoic acids (following Taylor, 2011). Horizontal bands represent OM-poor (pale grey) and OM-rich (medium grey) Waipawa organofacies.**

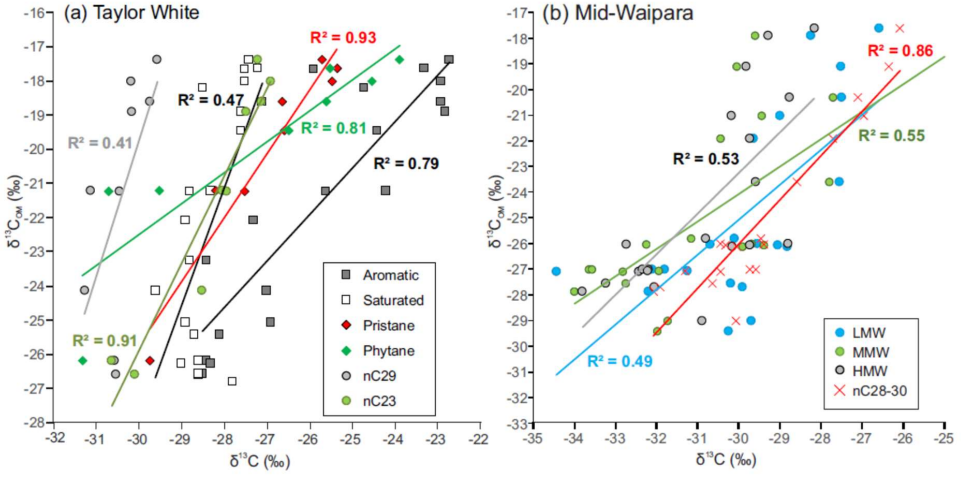

Figure 10. Correlation of $\delta^{13}C_{OM}$ with representative compounds at (a) Taylor White and (b) mid-Waipara sections. See Figure 9 caption for explanation of abbreviations.

https://doi.org/10.5194/cp-2021-122
Preprint. Discussion started: 17 September 2021

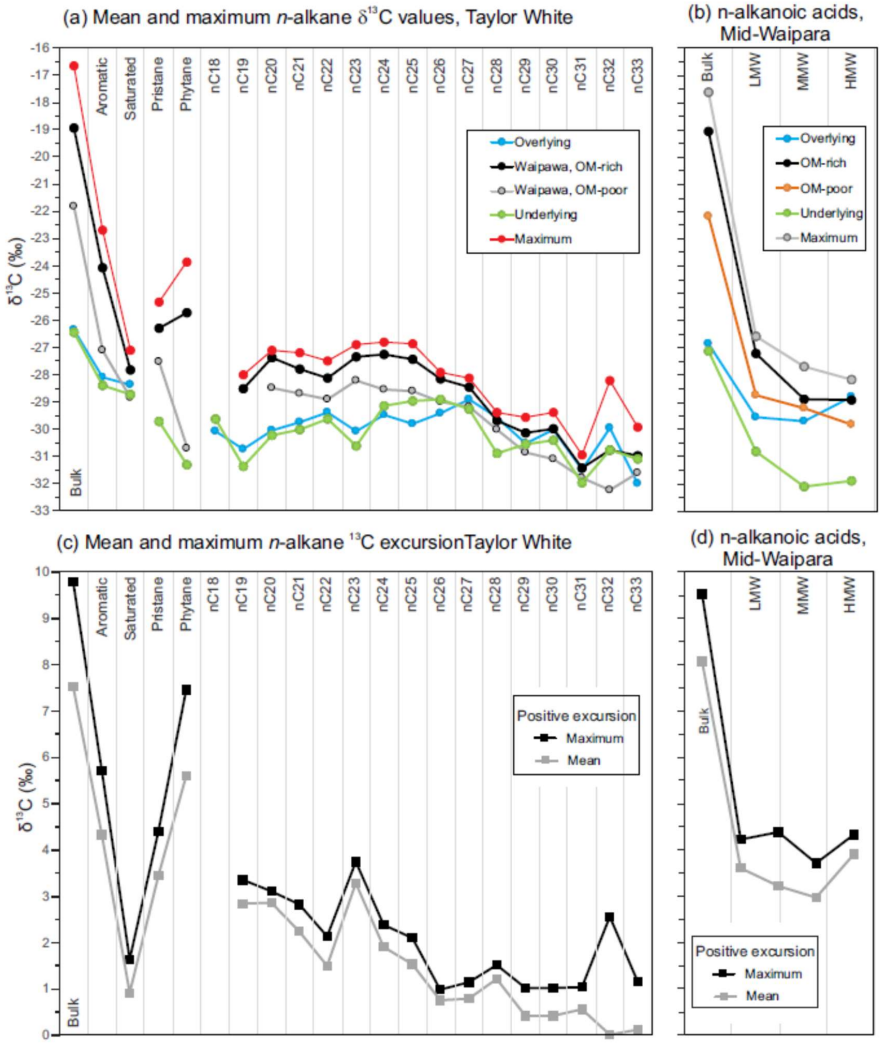

950

Figure 11. Mean compound group and compound-specific $\delta^{13}C$ values for the four facies (underlying, overlying, OM-rich and OM-poor Waipawa) and maximum values for Waipawa organofacies in the (a) Taylor White and (b) mid-Waipara sections and mean and maximum positive $\delta^{13}C$ excursion values for the (c) Taylor White and (d) mid-Waipara sections. The excursion values were derived by subtracting OM-rich Waipawa mean and maximum values from mean values for the underlying facies.

https://doi.org/10.5194/cp-2021-122
Preprint. Discussion started: 17 September 2021

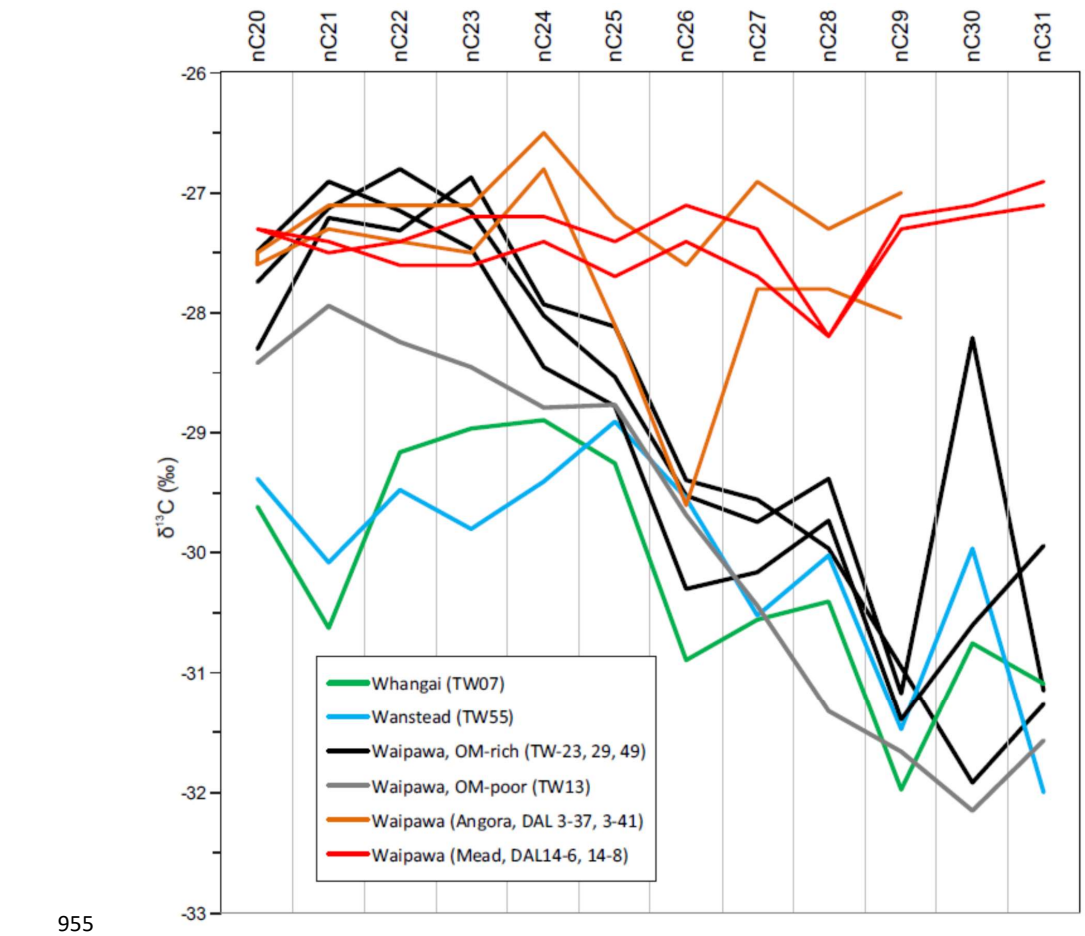

955

Figure 12. Compound-specific $\delta^{13}C$ profiles for representative samples from four marine organofacies (Wanstead, Whangai, OM-rich and OM-poor Waipawa) in Taylor White section compared to Waipawa organofacies at Angora Road and Mead Stream.

https://doi.org/10.5194/cp-2021-122
Preprint. Discussion started: 17 September 2021

Climate of the Past Discussions
Open Access
EGU

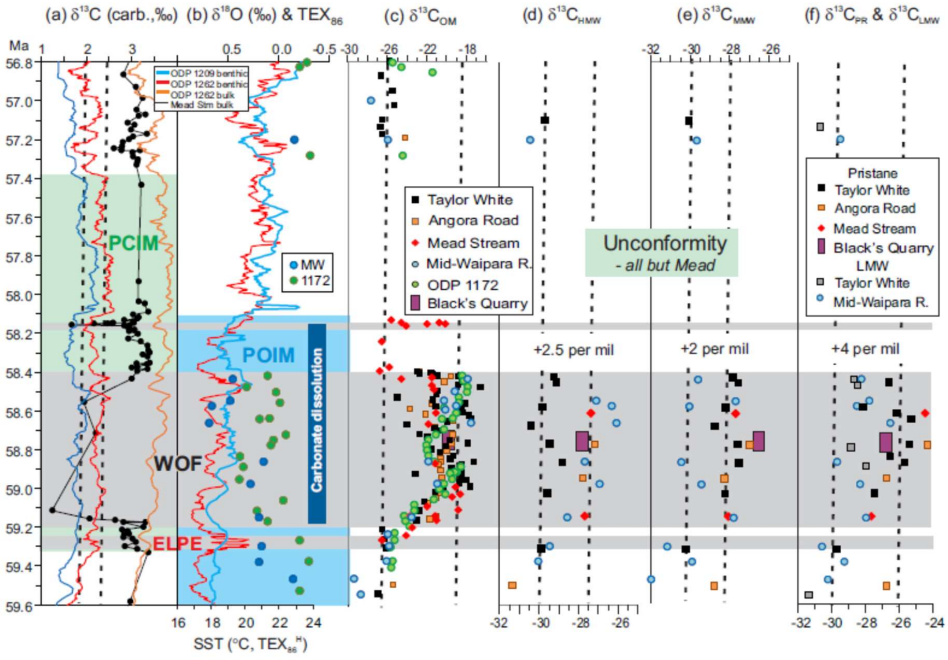

Figure 13. Summary of organic $\delta^{13}C$ variation in Waipawa and bounding organofacies from 59.5 to 56.8 Ma in comparison with the deep sea benthic foraminiferal and carbonate (a) $\delta^{13}C$ and (b) $\delta^{18}O$ (See Figure 1 for references). Local sea surface temperature (SST) estimates derived from the TEX_{86} proxy (Hollis et al., 2014; 2019; Taylor et al., 2018) are also shown in panel (b).Vertical dashed lines represent mean background values and mean values for the (a) Paleocene carbon isotope maximum and Waipawa organofacies for (c) bulk OM, (d) high molecular weight (HMW), (e) medium molecular weight (MMW) and (f) low molecular weight (LMW) *n*-alkanes, *n*-alkanoic acids and (f) pristane. For *n*-alkanes, LMW = C_{19}; MMW = C_{21}, C_{23}, C_{25}; HMW = C_{27}, C_{29}, C_{31}. For *n*-alkanoic acids, LMW = C_{16}, C_{18}; MMW = C_{20}, C_{22}, C_{24}, C_{26}; HMW = C_{28}, C_{30}. Age control for Taylor White, mid-Waipara and Mead sections and ODP Site 1172 based on biostratigraphic and magnetostratigraphic constraints combined with and correlation of the bulk carbonate $\delta^{13}C$ records at Mead Stream and ODP Site 1262 (See Supplementary Material S2). Only approximate ages for Angora Road and Black's Quarry samples are possible. Timescale is based on Gradstein et al. (2012).

https://doi.org/10.5194/cp-2021-122
Preprint. Discussion started: 17 September 2021

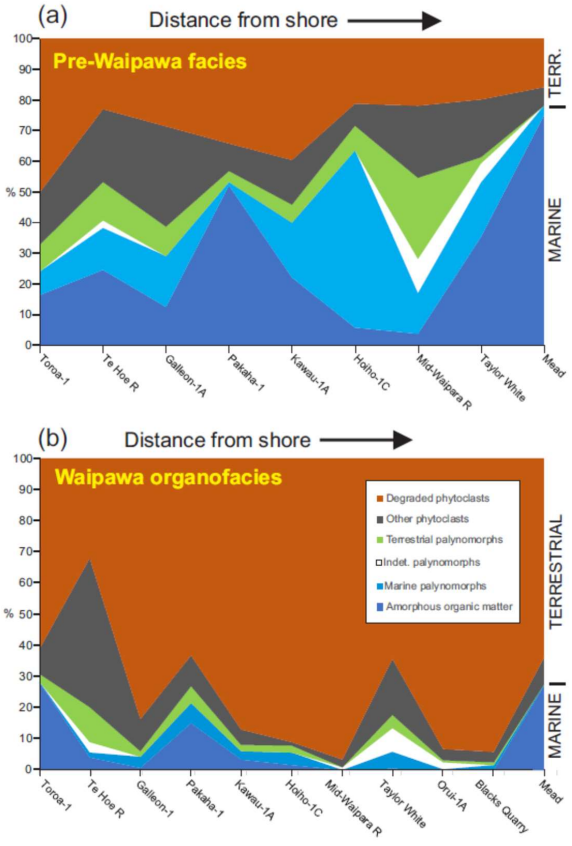

970 **Figure 14. Palynofacies variation in relation to inferred relative distance from shore for (a) Waipawa organofacies and (b) the underlying Whangai or correlative facies, based on mean values. See Table S1 for paleodepth assessments for each locality.**

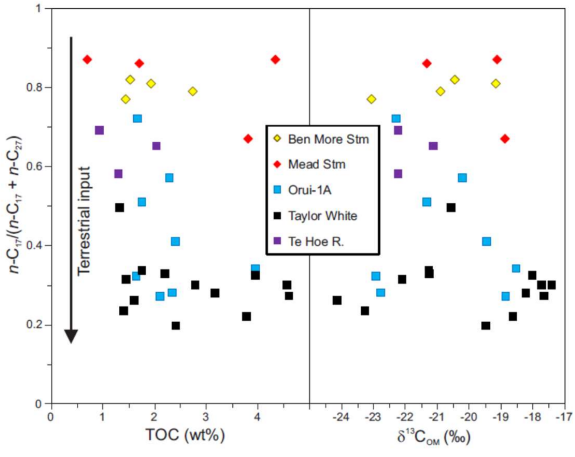

Figure 15. Relative abundance of C_{17} *n*-alkanes in relation to (a) TOC and (b) $\delta^{13}C_{OM}$ as a guide to aquatic/marine input in
975 **Waipawa organofacies at five sections representing a middle shelf to middle slope transect: Te Hoe River → Taylor White → Orui-1A → Mead Stream → Ben More Stream.**